Planetary and Space Science 60 (2012) 34–51

Contents lists available at ScienceDirect

Planetary and Space Science

journal homepage: www.elsevier.com/locate/pss

Titan's fluvial valleys: Morphology, distribution, and spectral properties

M.H. Langhans [a,*], R. Jaumann [a,b], K. Stephan [a], R.H. Brown [c], B.J. Buratti [d], R.N. Clark [e], K.H. Baines [d], P.D. Nicholson [f], R.D. Lorenz [g], L.A. Soderblom [h], J.M. Soderblom [c], C. Sotin [d], J.W. Barnes [i], R. Nelson [d]

[a] German Aerospace Center, Institute of Planetary Research Rutherfordstr. 2, 12489 Berlin, Germany
[b] Department of Earth Sciences, Institute of Geosciences, Remote Sensing of the Earth and Planets, Freie Universitaet Berlin, Germany
[c] Department of Planetary Sciences, 1629 University Boulevard, University of Arizona, Tucson, AZ 85721, USA
[d] Jet Propulsion Laboratory, California Institute of Technology, M/S 183-601, 4800 Oak Grove Drive, Pasadena, CA 91109, USA
[e] United States Geological Survey, Mail Stop 964, Box 25046, Denver Federal Center, Denver, CO 80225, USA
[f] Astronomy Department, Cornell University, Ithaca, NY 14853, USA
[g] Space Department, Planetary Exploration Group, Johns Hopkins University Applied Physics Lab, 11100 Johns Hopkins Road, Laurel, MD 20723, USA
[h] United States Geological Survey, 2255 N Gemini Drive, Flagstaff, AZ 86001, USA
[i] Department of Physics, University of Idaho, Engineering-Physics Building, Moscow, ID 83844, USA

ARTICLE INFO

Article history:
Received 31 August 2010
Received in revised form
9 December 2010
Accepted 31 January 2011
Available online 21 February 2011

Keywords:
Titan
Valleys
Methane
Cassini
VIMS
RADAR

ABSTRACT

Titan's fluvial channels have been investigated based on data obtained by the Synthetic Aperture Radar (SAR) instrument and the Visible and Infrared Mapping Spectrometer (VIMS) onboard the Cassini spacecraft. In this paper, a database of fluvial features is created based on radar-SAR data aiming to unveil the distribution and the morphologic and spectral characteristics of valleys on Titan on a global scale. It will also study the spatial relations between fluvial valleys and Titan's geologic units and spectral surface units which have become accessible thanks to Cassini-VIMS data. Several distinct morphologic types of fluvial valleys can be discerned by SAR-images. Dendritic valley networks appear to have much in common with terrestrial dendritic systems owing to a hierarchical and tree-shaped arrangement of the tributaries which is indicative of an origin from precipitation. Dry valleys constitute another class of valleys resembling terrestrial wadis, an indication of episodic and strong flow events. Other valley types, such as putative canyons, cannot be correlated with rainfall based on their morphology alone, since it cannot be ruled out that they may have originated from volcanic/tectonic action or groundwater sapping. Highly developed and complex fluvial networks with channel lengths of up to 1200 km and widths of up to 10 km are concentrated only at a few locations whereas single valleys are scattered over all latitudes. Fluvial valleys are frequently found in mountainous areas. Some terrains, such as equatorial dune fields and undifferentiated plains at mid-latitudes, are almost entirely free of valleys. Spectrally, fluvial terrains are often characterized by a high reflectance in each of Titan's atmospheric windows, as most of them are located on Titan's bright 'continents'. Nevertheless, valleys are spatially associated with a surface unit appearing blue due to its higher reflection at 1.3 μm in a VIMS false color RGB composite with R: 1.59/1.27 μm, G: 2.03/1.27 μm, and B: 1.27/1.08 μm; the channels either dissect pure bluish surface units or they are carved into terrain with a mixed spectral signature between bright and bluish surface materials. The global picture of fluvial flows clearly indicates a high diversity of parameters controlling fluvial erosion, such as climatic processes, as well as surface and bedrock types. Recent fluvial activity is very likely in the north polar region in contrast to more arid conditions at lower latitudes and at the south pole of Titan. This divergence is probably an indication of seasonal climatic asymmetries between the hemispheres. However, traces of previous fluvial activity are scattered over all latitudes of Titan, which is indicative of previous climatic conditions with at least episodic rainfall.

1. Introduction

The surface of Titan exhibits many putative fluvial features (referred to as channels or valleys) that have been revealed by Cassini imaging instruments, such as ISS (Porco et al., 2005), radar-SAR (Elachi et al., 2006; Lorenz et al., 2008), VIMS (Barnes et al., 2007b; Jaumann et al., 2008), and high-resolution DISR-data of the Huygens Landing Site (Tomasko et al., 2005; Soderblom et al., 2007b; Jaumann et al., 2009). Further evidence of fluvial processes on the surface of Titan was found at the Huygens Landing Site (HLS), where a number of rounded cobbles confirm the alluvial character of this particular area (Tomasko et al., 2005).

Given Titan's low surface temperature of 94 K, only methane (CH_4) and ethane (C_2H_6) will be in their liquid state (Lunine et al.,

* Corresponding author. Tel.: +49 30 67055398.
E-mail address: mirjam.langhans@dlr.de (M.H. Langhans).

0032-0633/$ - see front matter © 2011 Elsevier Ltd. All rights reserved.
doi:10.1016/j.pss.2011.01.020

1983; Flasar, 1983; Lorenz et al., 2002). Methane is the only substance known to participate in a volatile cycle due to its high vapor pressure that allows evaporation, condensation, the formation of clouds, and rainfall (Lorenz and Lunine, 1996; Lorenz et al., 2003, 2008; Atreya et al., 2006, 2009). Fluvial erosion on Titan's surface results from the action of this volatile cycle. Similarly to erosion by water on Earth, liquid methane may have shaped the surface of Titan in a characteristic way, primarily through mechanical erosion (Ori et al., 1998; Perron et al., 2006). It can thus be assumed that the existing rich diversity of channels and valley types has developed as a result of precipitation and subsequent erosion by liquid methane and possibly more complex hydrocarbons (Tomasko et al., 2005; Perron et al., 2006; Soderblom et al., 2007b; Komatsu, 2007; Lorenz et al., 2008; Jaumann et al., 2009). Many valley systems are arranged in the form of hierarchical and dendritic networks, suggesting that they are most likely of pluvial–fluvial origin (Mangold et al., 2004; Lorenz et al., 2008; Jaumann et al., 2009). A further indication supporting the assumption that the valleys were formed by rainfall is Titan's low number of craters with diameters between 20 and 100 km, indicative of intense resurfacing processes (Porco et al., 2005; Elachi et al., 2006; Jaumann et al., 2009; Wood et al., 2010). Despite some fundamental difference in boundary conditions on Titan and Earth (such as lower temperature and gravitation, higher atmospheric pressure on Titan), different substances involved in the volatile cycles, and different bedrock materials (such as silicates on Earth, icy materials on Titan), the physical effect of fluvial erosion, determined by the rate of bedrock incision, sediment transport and erosion, is expected to range within the same order of magnitude (Collins, 2005; Burr et al., 2006; Jaumann et al., 2009).

Many uncertainties remain regarding Titan's climatic and geologic background as well as any interactions between atmosphere and surface. Pre-Cassini studies suggested lower rainfall rates and a weaker erosional potential than that of Earth (Lorenz and Lunine, 1996), which is supported by observations by the recent Cassini mission, which indicated a rather dry climate, most pronounced at low latitudes (Radebaugh et al., 2008; Lunine and Atreya, 2008). To explain the ubiquity of fluvial features, occasional violent rainstorms are proposed, forming wadi-like channels, akin to processes in terrestrial deserts (Lorenz, 2000; Hueso and Sánchez-Lavega, 2006). Alternatively, founded on in situ data on temperatures and atmospheric methane concentrations, Tokano et al. (2006) proposed a steady methane drizzle.

A number of earlier studies focussed on the analysis of individual fluvial channels or fluvial systems based on VIMS and radar data, e.g. to deduce the rates of methane precipitation, transportation, and sedimentation (Jaumann et al., 2008; Perron et al., 2006) or on the origin and chemical composition of the flowing medium (cf. Elachi et al., 2006; Barnes et al., 2007b). A comprehensive global investigation, including the overall distribution of valleys as well as their spectral and morphologic characteristics is still outstanding. A first attempt at this will be made in the present paper, hoping that a detailed analysis will shed more light on the geologic interplay between fluvial and other geologic features. Investigating fluvial features provides insights into climatic conditions since the valleys serve as a record for rainfall events in the past and even for more recent climatic conditions. The findings presented will be set into relation to recent atmospheric models and observations. In order to derive any propositions regarding Titan's climatic background it is crucial to distinguish between valleys of a clear precipitation origin and valleys of an uncertain origin and development. In this context, the valley morphology or the arrangement of channels provides essential clues. A dendritic network geometry is highly suggestive of a development from atmospheric rainfall and rules out any origin from volcanic action or geologic faulting/rifting. Furthermore, studying the valleys' morphological characteristics can help understand the regional or local topography and the characteristics of surface and bedrock (Burr et al., 2009). This analysis is complemented by spectral investigations of fluvial terrains based on VIMS data. Thus, the global investigation of fluvial landscapes presented in this paper expands our knowledge on climatic, geologic, and topographic conditions on Titan, showing a non-trivial global picture of Titan's valleys.

2. Database and processing of the data

Image data from the radar SAR and the VIMS instrument onboard the Cassini spacecraft have provided the database for the present study. VIMS data enable complementary research into the spectral properties of Titan's surface, covering a spectral range from 0.35 to 5.2 μm (Brown et al., 2006) at spatial resolutions between a few kilometers down to 250 m per pixel (Jaumann et al., 2009). Owing to Titan's dense atmosphere, only few atmospheric windows within the near-infrared wavelength range are sensitive to surface features; thus, VIMS must rather be regarded as a multi-spectral sensor (Jaumann et al., 2006). Atmospheric windows are centered at 0.94, 1.08, 1.28, 1.6, 2.0, 2.8, and 5.0 μm (Brown et al., 2006; Barnes et al., 2007a; Clark et al., 2010). VIMS data permit a distinction between three broad spectral surface types based on slight but distinct spectral differences. The spectral variability of the surface is represented by false-color spectral composites, e.g. in ratio composites with R: 1.58/1.28 μm, G: 2.0/1.28 μm, and B: 1.28/1.08 μm, depicted in Fig. 6 of Jaumann et al. (2008). Three surface types are revealed, namely bright, dark brown, and dark blue surface units (Porco et al., 2005; Barnes et al., 2007a; Soderblom et al., 2007a; Le Mouélic et al., 2008; Jaumann et al., 2008, 2009; Stephan et al., 2009). The differentiation into surface units can be the result of a particular different composition of materials or, alternatively, of different grain sizes (McCord et al., 2006; Soderblom et al., 2007a, 2009; Le Mouélic et al., 2008; Clark et al., 2010). In either case, revealing the processes that lead to the particular stratification of Titan's surface provides important clues to understand Titan's geology.

A global Cassini VIMS mosaic formed the basis for a spectral investigation of Titan's low latitudes. The VIMS-data utilized were obtained between October 2004 and December 2008 (see Table 1).

Table 1
Specifications of the VIMS-observations utilized in this work (from Barnes et al., 2009b, modified).

Flyby	Date	Best spatial sampling (km)
Ta	October 26, 2004	2.6
Tb	December 13, 2004	1.35
T4	March 31, 2005	1.2
T8	October 28, 2005	42
T9	December 26, 2005	2.9
T10	January 15, 2006	3.9
T11	February 27, 2006	18
T12	March 18, 2006	7
T13	April 30, 2006	10
T17	September 7, 2006	7.5
T20	October 25, 2006	0.49
T28	April 10, 2007	11
T31	May 28, 2007	11
T32	June 13, 2007	12
T33	June 29, 2007	12
T34	July 19, 2007	8
T35	August 31, 2007	10
T38	December 5, 2007	0.33
T40	January 8, 2008	1.95
T42	March 25, 2008	10
T48	December 5, 2008	14.2

The VIMS cubes were transformed into a simple cylindrical projection (centered at 180°W) with a spatial resolution of 10 km per pixel. Resampling was performed using the nearest-neighbor algorithm in order to maintain the original spectral information (Jaumann et al., 2006; Stephan et al., 2009). VIMS mosaics with deficient ground resolution, poor signal-to-noise-ratio and/or unfavorable illumination conditions were excluded following Stephan et al. (2009). Beyond the equatorial region (latitudes $>30°$N and $>30°$S) the VIMS coverage and/or ground resolution is currently not adequate for a comprehensive spectral analysis. Ratio-composites of wavelength bands within Titan's atmospheric windows were created (R: 1.58/1.28 μm, G: 2.0/1.28 μm, B: 1.28/1.08 μm) to highlight the overall spectral variations. This VIMS composite of Titan's lower latitudes was used for visual mapping of the three spectral units.

The radar instrument images Titan's surface in SAR mode (Synthetic Aperture Radar) at spatial resolutions between 0.3 and 1.5 km per pixel (Elachi et al., 2004), allowing the identification and mapping even of small-scale features. This paper is based on radar data obtained between October 2004 and June 2009 (T00A to T057) (see Table 2). Currently, radar swaths cover nearly 40% of Titan's surface. SAR-data of the lower and mid-latitudes were processed and reprojected into a simple cylindrical projection, centered at 180°W, using the USGS image processing program ISIS (Integrated Software for Imagers and Spectrometers). Polar maps were created following the same preprocessing steps, using the polarstereographic projection. Radar and VIMS data are stored and processed in the ArcGIS software environment provided by ESRI (Environmental Systems Research Institute).

Table 2
Characteristics of the RADAR-SAR swaths utilized in this work.

Orbit	Date	Altitude (km)	Latitude range (deg)	Longitude range (deg)	Incidence angle (deg)
TA	October 26, 2004	1200	32–53N	10–130W	2–46
T3	February 15, 2005	950	2S–22.5N	0.4–133W	1–30
T7	September 07, 2005	950	25–75S	23–350W	7–35
T8	October 28, 2005	450	7–11S	186–314W	1–31
T13	April 30, 2006	1850	3–18S	60–172W	10–29
T16	July 22, 2006	950	13–90N	138–358W	9–40
T17	September 07, 2006	950	5–14N	33–68W	29–45
T18	September 23, 2006	950	15–65N	105–346W	19–45
T19	October 09, 2006	950	2S–42N	160–318W	9–39
T21	December 12, 2006	950	25S–50N	195–290W	9–57
T23	January 13, 2007	950	35S–53N	95–335W	9–39
T25	February 22, 2007	953	33S–62N	215–55W	8–39
T28	April 10, 2007	951	18S–62N	5–37W	6–36
T29	April 26, 2007	951	4S–90N	195–360W	0–38
T30	May 12, 2007	950	35–68N	225–325W	9–48
T36	October 02, 2007	950	35–77S	24–196W	30–61
T39	December 20, 2007	953	26–89S	13–220W	9–55
T41	February 22, 2008	959	16N–45S	53–220W	2–41
T43	May 12, 2008	950	32N–37S	73–219W	8–41
T44	May 28, 2008	1320	25N–35S	93–225W	8–26
T48	December 05, 2008	3575	53N–34S	94–239W	11–75
T49	December 21, 2008	3575	31N–72S	207–280W	8–39
T50	February 07, 2009	3575	18N–61S	293–17W	30–59
T55	May 21, 2009	965	39N–76S	120–285W	10–39
T56	June 6, 2009	965	31N–73S	129–319W	9–39
T57	June 22, 2009	955.5	19N–85S	127–330W	30–75

3. Methodology

A global valley database has been developed based on radar-SAR. The key criteria for identifying linear topographic depressions as valleys according to Lorenz et al. (2008) and Burr et al. (2009) are the presence of a linear shape with a substantial contrast to the surrounding terrain, a typical bright/dark pairing resulting from the topographic incision of the channel, and a morphological resemblance to terrestrial rivers, i.e. their arrangement in hierarchical branching networks. Based on the current radar coverage of nearly 40% at a resolution of 350 m/pixel, about 22,300 km of river channels were identified and mapped. The resulting map of fluvial valleys of Titan's lower and mid-latitudes is depicted in Fig. 1. In order to gain a deeper understanding of fluvial flow on Titan, descriptive data on the particular fluvial features were studied, such as their length, width, morphological characteristics, and the complexity of the network as determined by their drainage pattern. Stream order labels were used to mark the number of tributaries counted upstream from the receiving stream (Butzer, 1976; Ahnert, 2003).

The GIS-based database of fluvial features on Titan offers tools to assess the geometric dimensions (such as lengths and widths) of linear features. These dimensions are relevant for comparisons with Martian and terrestrial valleys as well as to estimate the channels' discharge volumes. The length of fluvial valleys can be determined automatically. Estimating the width of a valley is made difficult by the fact that the lateral extension of most of these features is small, i.e. near the spatial resolution of the radar instrument. The bright/dark pairing of deeply incised fluvial channels caused by certain observation geometries results in unknown fractions of the valley escarpment and valley floor being hidden by the radar shadow. Further uncertainties arise from the fact that the interior channel, which has experienced fluid flow (referred to as 'channel'), and the surrounding eroded valley occupied by the channel (referred to as 'valley') are often hard to distinguish (Perron et al., 2006; Jaumann et al., 2008). It must be assumed that the linear features visible in radar images represent the overall extension of the entire valley rather than that of the interior channel. Therefore, gathering morphological information is complicated, geometric measurements (i.e. the width of the riverbed) can be imprecise, and calculations of channel discharges provide only upper limits. However, SAR data provide an overview of the geometric dimensions of Titan's valleys and permit comparing Titan's valleys to those on Mars and Earth.

Generally, extended high-contrast linear features can be recognized even if their width is below the image resolution (Schowengerdt, 1997; Barnes et al., 2007b). However, it is not possible to assert the minimum size of an object detectable by radar, since its visibility depends on intrinsic physical and morphological properties of the object and its surroundings (such as composition, slope, and roughness of the surface) as well as on the viewing geometry and the ground resolution at that specific location. Generally, reasonable minimum sizes which are necessary to securely identify an object as a discrete entity range between the size of one pixel and up to 3×3 pixels (Knight and

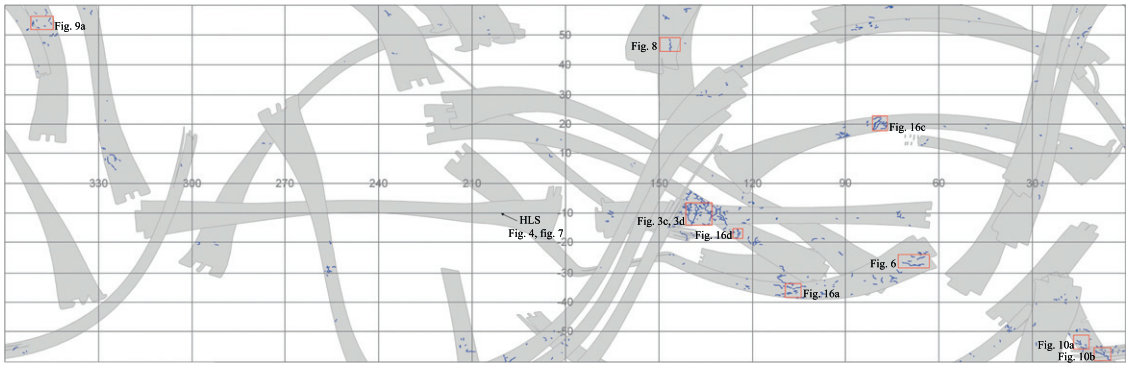

Fig. 1. Map of fluvial valleys (highlighted in blue) on Titan. Radar coverage is shaded in gray. Simple cylindrical projection of Titan's lower and mid-latitudes. Red boxes indicate the locations where the close-view images were taken.

Fig. 2. Cassini-image database in a global view. Simple cylindrical projection of lower and mid-latitudes. Radar observations from October 2004 through June 2009 with ground resolutions between 0.3 and 1.5 km per pixel. Background: VIMS observations (reflectance at 2 μm) from TA through T48 (October 2004 to December 2008) resampled to a ground resolution of 10 km.

Lunetta, 2003). If one defines valleys as extended linear features it is plausible to expect their minimum width required for a secure identification to be below the pixel size, since linear features can be recognized even through a series of mixed pixels (Barnes et al., 2007b).

A combined investigation of fluvial valleys and their spectral properties was facilitated by integrating them into the GIS software, given the same map projection of both datasets. VIMS data shed light on the composition of the upper cm or mm (Clark et al., 2010) of the surface (often with a significant contribution by the atmosphere to the captured signal), while the radar signal is not impaired by the atmosphere and reflects the character of the surface from a more physical perspective (e.g. surface roughness). Radar-SAR penetrates the upper centimeters up to 10 m of the surface (Elachi et al., 2004). Thus, the two datasets are not necessarily comparable and there is hardly any correlation between them (Soderblom et al., 2007a; Le Mouélic et al., 2008). On the other hand, data provided by the two instruments are not redundant, and help investigate the surface properties in two different ways. A global view of Titan's low and mid-latitudes composed from VIMS and radar databases is shown in Fig. 2.

4. Morphology

In the following, a broad classification of fluvial valleys is given, which is mainly based on morphologic properties but also considers the ambient environmental conditions. That is, valleys with morphologies pointing to similar boundary conditions (such as the climate) were combined into a singular valley class, irrespective of differences in morphology.

Two channel (-systems) obtained from Wall et al. (2010) and Paganelli et al. (2005) could not be assigned to any specific channel class. These are the 'fan-like' and the 'flooded' channel, see Table 4. The two denotations are adapted from the literature.

Generally, any geologic interpretation is complicated by the fact that different geologic processes can result in similar landforms (known as the concept of equifinality according to von Bertalanffy, 1968). This principle is highly relevant for Titan's surface since many geologic features are at or even beyond their resolution limit of 350 m per pixel of the radar-SAR sensor. Therefore, the origin of some valleys remains ambiguous since the linear shape of valleys is not uniquely attributable to fluvial flow caused by precipitation. Linear landforms can also form as a result of volcanic or tectonic action (geologic faulting/rifting), or be caused by erosion through subsurface liquids. In order to identify the process causing the formation of a particular landform, its morphology and geometry are essential. The degree of certainty as to their development from rainfall is discussed in this section for each of the valley types separately. A global map including Titan's recent nomenclature is shown in Stephan et al. (2009).

4.1. Dendritic valleys

Titan's most evident valleys are arranged in integrated dendritic networks. Dendritic valley systems form tree-shaped networks with many contributing branches that converge into larger receiving streams. Besides valleys modified by glacial

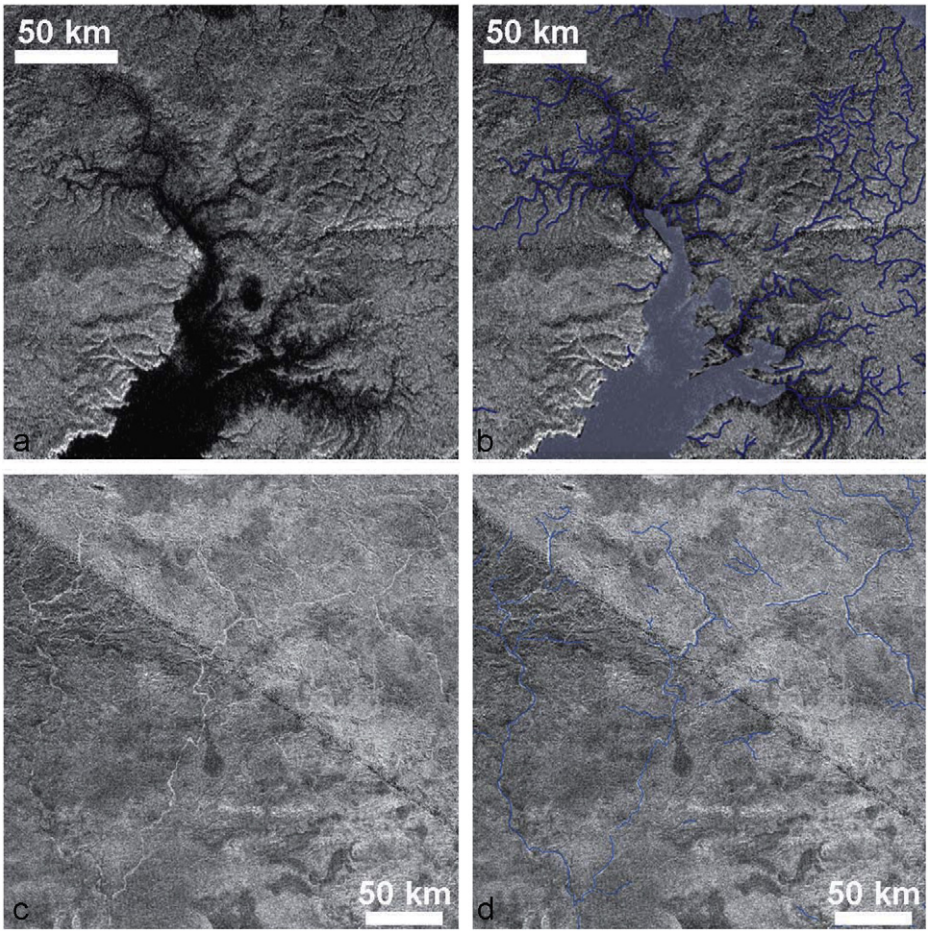

Fig. 3. (a) Dendritic valley network at high northern latitudes, ending in Kraken Mare, captured by radar-SAR (T28, April 10, 2007) centered at 280°W, 78°N (course of the valleys is delineated in (b)). (c) Dendritic valley network on Xanadu, captured by radar-SAR (T13, April 30, 2006) centered at 138°W, 10°S. (course of the valleys is delineated in (d)).

processes, dendritic valley networks constitute the most common type of drainage systems on Earth, featuring a V-shaped cross-section and situated on less permeable or impermeable bedrock (Williams and Phillips, 2001; Sahlin et al., 2009). Meanders are prevalent in areas without substantial stream flow variations. These unstable landforms adjust to discharge variations through increase/decrease of meander wavelength and wave amplitude (Butzer, 1976). Meandering of channels can be regarded as a morphological counterpart to braiding of channels, which becomes manifest in frequent shifts and relocations of the riverbed caused by high variations in stream flow (Butzer, 1976).

The morphological characteristics of dendritic systems on Earth can broadly be confirmed for Titan's dendritic channels. Titan's most prominent dendritic networks are situated near Titan's north pole (see Figs. 3a and b) (Stofan et al., 2007; Mitchell et al., 2007), at low latitudes, for example at western Xanadu (see Figs. 3c and d) (Barnes et al., 2007b; Lorenz et al., 2008), and at the Huygens Landing Site (HLS) (see Fig. 4) (Tomasko et al., 2005; Perron et al., 2006; Soderblom et al., 2007b).

Dendritic networks cover large areas near the equator, both on a local scale (near the HLS) and on a regional scale (Xanadu's channels). Western Xanadu as well as the north polar region exhibit very complex, meandering, and extended dendritic valley networks. Dendritic valleys near the HLS (see Fig. 4) are unique regarding their spatial extension resolved by the DISR imager (Tomasko et al., 2005; Perron et al., 2006; Soderblom et al., 2007b). Here, only a small fraction of Titan's surface is covered by very narrow channels emerging on bright highlands and

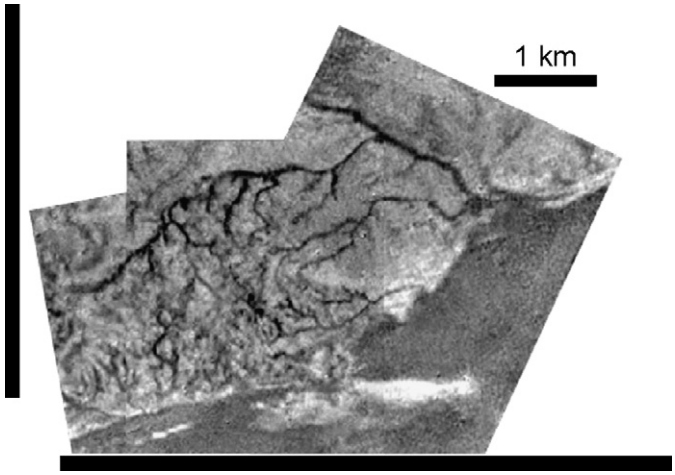

Fig. 4. Dendritic valley network at the Huygens Landing Site, captured by the DISR High and Medium Resolution Imager, panoramic mosaic (January 14, 2005). Image is centered at 192°W, 10°S (from Tomasko et al. (2005), modified).

directed toward darker lowlands. The sharply defined albedo boundary is interpreted to be a 'coastline' of a former terminal sea or lake which has meanwhile run dry (Tomasko et al., 2005; Soderblom et al., 2007b). The widths of the channels obtained by DISR vary between 17 and 250 m, at a length of up to 15 km of the main receiving stream (Perron et al., 2006; Jaumann et al., 2008,

2009). Xanadu's channels measure several hundreds of kilometers (the longest exceeding 450 km), with widths varying between 350 up to about 2500 m. Valleys near the north pole have widths between the resolution limit of the radar instrument of 350 m up to 5 km, broadening where the valley opens out into the sea, at a length of up to 250 km (see Table 4).

Dendritic valleys are either radar-bright (e.g. those at western Xanadu, Figs. 3c and d) or radar-dark (e.g. those near the north pole, Figs. 3a and b). The strength of the radar return depends among other factors on the roughness of the reflecting surface (Elachi et al., 2006), thus, it is to some extent possible to evaluate whether a particular channel has a smooth surface or not. Low radar backscatter is caused by materials that are smooth at the radar wavelength of 2.17 cm. A smooth surface can result from a deposition of fine-grained sediments, indicative for slower-moving flows or even for the presence of an open body of liquids (Lorenz et al., 2008). Radar-bright channels are interpreted to be covered by coarser sediments, such as rounded icy blocks (Le Gall et al., 2010). However, the intensity of the radar return depends upon several factors other than the roughness and surface structure, such as the layering, surface slope, inclination, composition, volume scattering, and dielectric constant of the material (Thompson and Squyres, 1990; Elachi et al., 2006; Kirk et al., 2007) so that clear correlations between the signal strength and the roughness/smoothness or even the recent activity of the channel are not necessarily implied. Nevertheless, one can make at least relative or comparative statements about the channel floor relative to its surroundings or between different channels.

With a high level of certainty the valleys close to the north pole are currently filled, due to the very low radar backscatter of their interior channels (see Figs. 3a and b). Many of the valleys at high northern latitudes drain into lakes. These lakes are likewise interpreted to be filled with liquids due to their characteristic shape and their low radar return (Stofan et al., 2007). This hypothesis is supported by spectral investigations based on VIMS data (Brown et al., 2008; Stephan et al., 2010) and analyses of the radar echo that showed their surface to be extremely smooth, with elevation differences below 3 mm (Wye et al., 2009). Since the valleys surrounding the lakes have a similarly low radar backscatter, this is also a very likely indication of recent activity. These valleys have numerous interconnections and a well-defined course (Fig. 3a), which is a sign of a substantial topographic depression caused by fluvial incision.

By contrast, the valleys within the dendritic systems of western Xanadu have a high radar return. Those valleys are certainly not liquid filled and presumably covered by material with fragment sizes larger than the radar wavelength, possibly in the form of rounded rocks or pebbles (Le Gall et al., 2010).

The dendritic drainage systems near the north pole and at western Xanadu are located on – or are at least surrounded by – mountainous terrain. Topographic models of the valley system near the HLS revealed a rugged topography with a peak-to-peak relative topography variation of about 200 m and steep slopes of up to 30° (Tomasko et al., 2005; Soderblom et al., 2007b; Jaumann et al., 2009). The overall slope of the terrain can be deduced from the network geometry of the system. In the case of dendritic systems near the equator (see Fig. 3) the receiving streams are mainly directed southwards. The north-polar valleys have different flow directions, as almost each of them directly or indirectly ends in one of the numerous lakes, acting as local sinks. The channels at the HLS are oriented in south-eastern directions.

Valleys of the dendritic type most likely develop as a result of precipitation since they require a distributed rather than a local source of liquids (Mangold et al., 2004; Tomasko et al., 2005; Perron et al., 2006; Soderblom et al., 2007b; Lorenz et al., 2008; Jaumann et al., 2009). The high branching complexity with network orders of up to sixth or seventh (western Xanadu, see Table 4) is an indication for an origin from rainfall. The enormously extensive areas covered by dendritic systems as well as the length of the valleys (often exceeding several hundreds of kilometers) at relatively narrow widths argue against a development from spring-fed flows or sapping of subsurface liquids. The latter would require an extensive subsurface methane table to enable widespread seepage erosion, a precondition that is difficult to explain without precipitation and infiltration over a long period of time. Furthermore, the location of most of the dendritic networks within rugged and most likely elevated terrain argues against the presence of a shallow subsurface methane table as it would more likely be found in lowlands or even in topographic depressions. Thus, a formation through sapping is unlikely and a formation by pluvial/fluvial processes is the most probable explanation for dendritic channels (Tomasko et al., 2005; Perron et al., 2006; Soderblom et al., 2007b; Lorenz et al., 2008; Jaumann et al., 2009).

The location of dendritic valleys within or close to mountainous terrains suggests but not necessarily requires a development from or contribution by orographic rainfall (Lopes et al., 2010; Barth, 2010). For Xanadu's valleys, it is likely that although the recent climatic conditions are predominantly dry, precipitation in the past played a significant role. Both, the reason and the timescales for that climate change in this region remain unknown.

Due to their high complexity and the lack of impact craters in the neighborhood of dendritic valley systems, dendritic networks must be among the oldest fluvial systems on Titan, although their absolute age cannot be determined. On Earth, the absence of tectonic or lithologic influences, often observed in dendritic systems, points to a relatively old age (Ahnert, 2003). Meanders develop on fine-grained material, at relatively slight slopes of the terrain and at steady flow over a considerable time (Butzer, 1976). On the other hand, Burr et al. (2009) make a case for the influence of tectonism, given the geometric alignment of Xanadu's valleys. Tectonic control is also evident at the HLS due to the proposed steep slopes of the terrain and substantial incision of the channels (Tomasko et al., 2005; Soderblom et al., 2007b; Jaumann et al., 2009). At Titan's north pole tectonics appear to have had a significant impact on the network geometry as the general shape of the valleys is rectilinear with sharp angular junctions, rather than sinuous (Figs. 3a and b). Thus, dendritic systems leave us with a conflicting impression, since their high stream order and complex geometry point to long development times while the high tectonic control rather indicates a relatively short persistence of fluvial erosion and/or a high resistance of the underlying bedrock.

4.2. Dry valleys

Several putative drainage networks can be found at Titan's surface that resemble desert washes, or wadis, on Earth (Lorenz et al., 2008), or Martian outflow channels. Despite the morphological diversity within this valley type, all putative dry valleys are summarized in this section on the basis of the (assumed) similarity of the climatic conditions that have brought about these physiographies.

Some of Titan's dry valleys appear as broad and straight streams, sometimes rather similar to laminar surface runoff (see Fig. 5) unlike the linear, channelized flow in valleys. The boundaries between the interior channel and the entire negative relief of the dry valley cannot be distinguished, and even the valley escarpments are not perceptible due to the low contrast between the river bed and its surroundings in radar images. Flat cross-sections of the valleys are therefore expected (Lorenz et al., 2008) as opposed to the deeply incised, often V-shaped valleys of

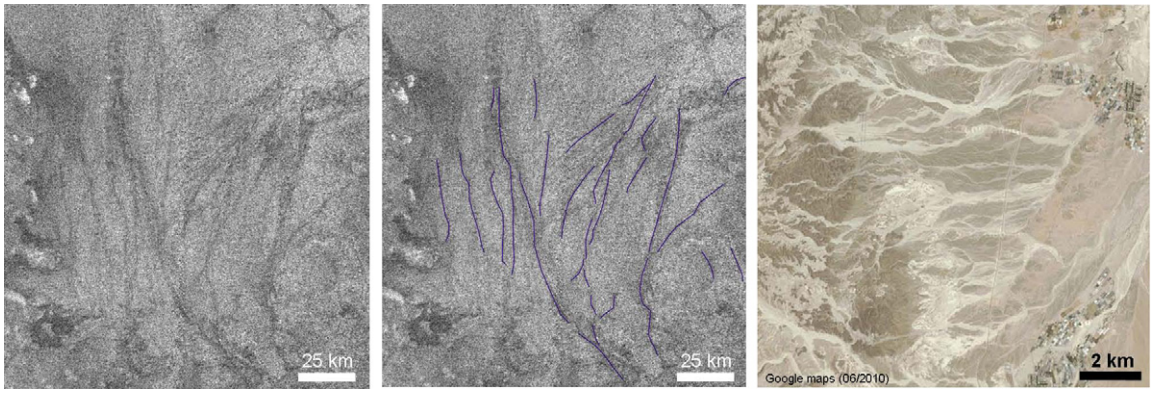

Fig. 5. Left: dry valleys from radar observation T7 (September 07, 2005). Image is centered at 7°W, 59°S. The putative course of the channels is delineated in the middle image. Right: terrestrial wadi-network. True-color image, centered at 30°45N, 35°13E (Israel). Similar to dry valleys on Titan, these valleys appear broad, flat and are not active at the time of image acquisition.

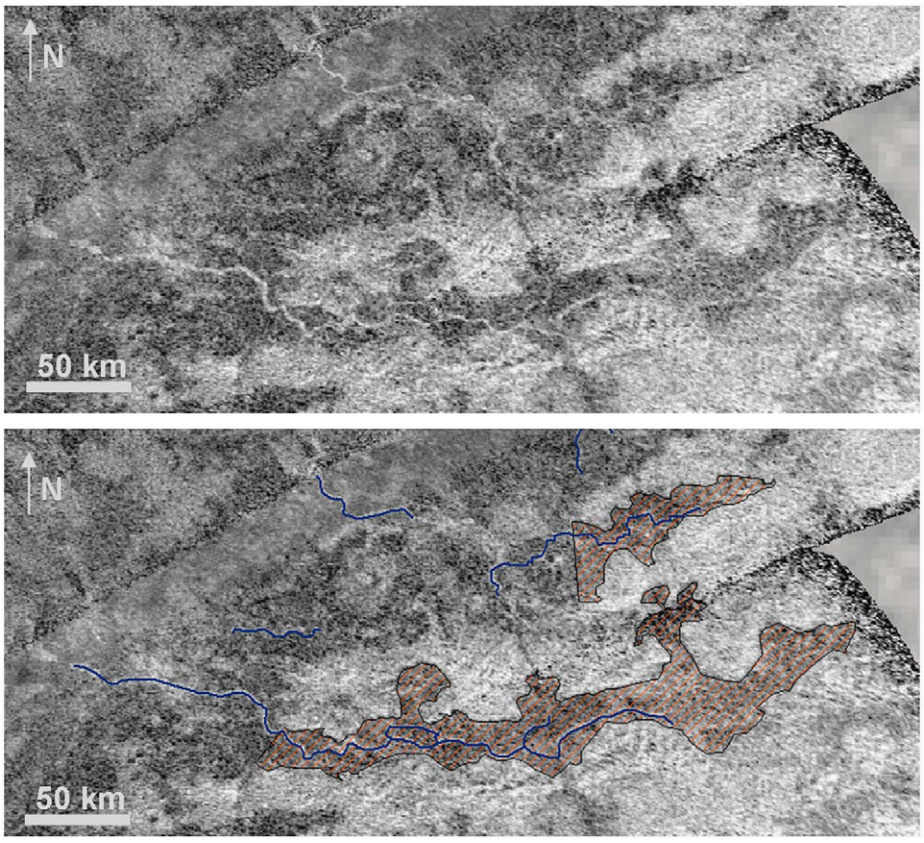

Fig. 6. Putative floodplains surrounding the interior channel. Top: radar observation (T41, February 22, 2008), image is centered at 67°W, 27°S. Bottom: radar image with interior channel marked in blue, floodplains are highlighted in red (striped).

the dendritic type (Williams and Phillips, 2001; Tomasko et al., 2005; Sahlin et al., 2009) (cf. Section 4.1). Dry valleys seldom exhibit meanders and are generally straighter, sometimes braided (see Fig. 5 and Elivagar Flumina channel system, Fig. 3 in Lorenz et al., 2008) possibly due to an ephemeral discharge regime. Episodic discharge of terrestrial and Martian valleys often entail braided and anastomosing patterns and fractions of residual uplands left within the riverbed (Baker, 2001).

Dry valleys on Titan are generally shorter and broader than valleys integrated within dendritic networks, with lengths of up to 300 km and widths up to 8 km (see Fig. 5 and Table 4).

Dry valleys are found in plain environments mainly at mid-latitudes (see Fig. 5, and in the Elivagar Flumina channel system, Fig. 3 in Lorenz et al., 2008). In contrast to dendritic fluvial systems, terrains covered by dry valleys are less extensive, and distributed only over a small proportion of Titan's surface.

Furthermore, some channels border on homogeneous and smooth terrain, which, in shape and texture, resembles that of floodplains (see outlines in Fig. 6). In this case, a relatively narrow radar-bright channel is surrounded by broad, relatively homogeneous radar-dark areas. Given their low radar-brightness, these putative floodplains are possibly covered by smooth sediments. Further, the presumed floodplains have relatively clear-cut boundaries with their surrounding, which in turn appear bright in radar. Interestingly, the valleys seem to vanish and the

channel course is no longer discernible at the left (western) image margin. Typical landforms of fluvial mouths, such as estuaries or deltas are not apparent. These morphological patterns argue for high variations in stream flow over a relatively short period, resulting in extended floodplains and high evaporation or infiltration due to the lack of receiving landforms. On the other hand, a smaller but steady discharge is required to explain the formation of the sharply defined interior channel. Compared with the dendritic channel system in the HLS area (Fig. 4), this network has a larger areal extent. The length of the main channel is about 350 km compared to 15 km length at the HLS. Both valley systems have a branching pattern with orders of tributaries of up to four (HLS) and two (Fig. 6), indicative of a fluvial/pluvial origin. Yet, the channels near the HLS do not exhibit any extended floodplains. This valley system is more consistent with an unchanging stream flow over time owing to the lack of floodplains.

The distribution of dry valleys observed is restricted to Titan's mid-latitudes. All of the dry valleys mentioned here appear bright in radar (at least the interior channel), supporting the idea of an episodic discharge regime with dry climatic conditions in recent times. In some cases the development of dry valleys from fluvial processes is relatively certain, while other features discussed here can also result from geologic processes, such as volcanic flow (see Fig. 5). Effusive lava flows with a low viscosity can result in laminar shapes (cf. Heslop et al., 1989). Due to the absence of diagnostic geologic features pointing to either of these processes, such as receiving lakes, seas, or coastlines suggesting fluvial origin, or calderas suggesting alternative volcanic origin, it is difficult to assess which process is responsible for the formation of this particular morphology.

Similar to terrestrial wadis, dry valleys on Titan are likely to have formed as a result of sudden, strong runoff events followed by long droughts (Lorenz et al., 2008), which is consistent with observations of ephemeral clouds and results of atmospheric models (Lorenz, 2000; Hueso and Sánchez-Lavega, 2006; Rannou et al., 2006; Jaumann et al., 2008; Rodriguez et al., 2009; Jaumann et al., 2009). Outflow events due to sudden melting of large volumes of ice account for broad, anastomosing and braiding flows on Mars (cf. Komar, 1979) but can be ruled out for Titan due to its environmental conditions that preclude glaciation (Lorenz and Lunine, 1996). It is conceivable, however, for at least some of the valleys assigned to this type to have been produced by geologic processes other than rainfall.

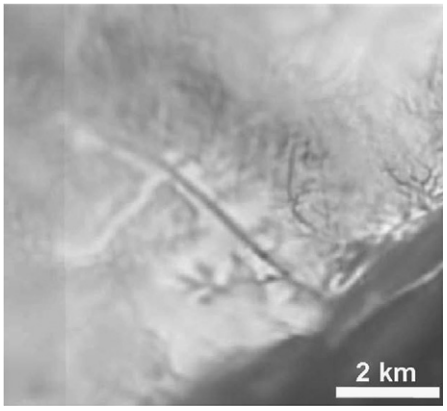

Fig. 7. Sapping channels from the DISR High and Medium Resolution Imager, panoramic mosaic (January 14, 2005). Image is centered at 10°S 192°W (from Tomasko et al. (2005), modified).

4.3. Sapping channels

It has been suggested that another process that may have sculptured Titan's surface is erosion by liquids emerging from the subsurface (Tomasko et al., 2005; Perron et al., 2006; Jaumann et al., 2009). Valleys created by sapping or seepage erosion tend to develop different morphologies compared to those formed by precipitation (Baker et al., 1990; Lamb et al., 2006), although there is no case in which a definite and exclusive origin from subsurface liquids has been confirmed, even on Earth and Mars (Lamb et al., 2006, 2008). Sapping channels are deeply incised, develop amphitheater-shaped heads and are generally shorter and broader compared to valleys formed by rainfall (cf. Howard and McLane, 1988).

Morphological indications of sapping through subsurface liquids can be found only at two locations on Titan so far. DISR data reveal a putative sapping network near the HLS (Tomasko et al., 2005) (see Fig. 7). Several branches converge at large angles with the receiving stream, which in turn drains southward toward what may be a coastline (Tomasko et al., 2005; Soderblom et al., 2007b; Jaumann et al., 2009). This valley system is very small, with lengths of the main channel below 15 km and widths up to 100 m (Jaumann et al., 2009). Another likely sapping landscape is revealed by radar data around 143°W, 50°N (see Fig. 8). The curvilinear features at this location resemble some deeply incised canyons on Earth (cf. Schumm et al., 1995) and have considerable lengthwise and lateral dimensions (width up to 5 km, the length of the system adds up to about 200 km, see Table 4) but the channels seem unconnected. The broad interior channels have a substantially lower radar return than the adjacent areas. Geometrically, the network is very simple as only some valleys drain into the larger putative terminal valley. In both cases, the channels are of a short and stubby shape

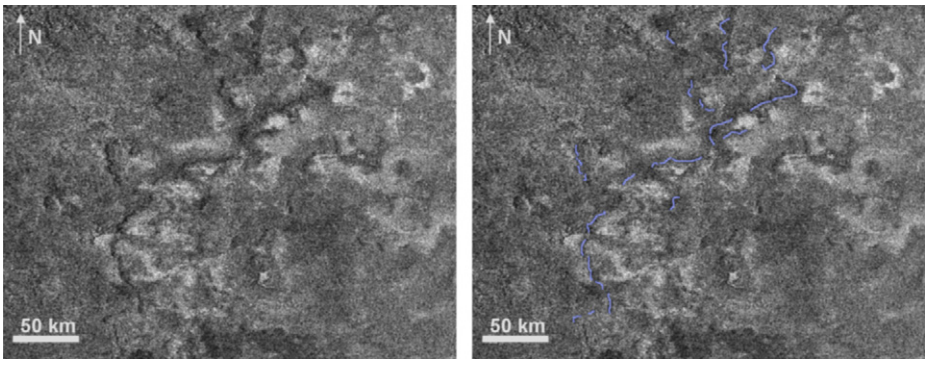

Fig. 8. Putative canyon system from radar observations, radar-SAR (T16, July 22, 2006). Image is centered at 143°W, 50°N. The presumed course of the canyons is highlighted in the right figure.

with large confluence angles between tributaries and receiving streams.

Although a fluvial origin is very likely, a definite contribution through subsurface liquids cannot be verified, especially in the case of Fig. 8. The observed features can also result from tectonic processes. Strong tectonic control and preferential erosion in given fissures combined with less resistant bedrock and steady rainfall might also explain the high angles of the tributary junctions in Fig. 8 (cf. Burr et al., 2009), although the sinuous shape of the branches is more consistent with fluvial flow. High tectonic control is also suggested by Jaumann et al. (2009) for the putative sapping landscape at the HLS (see Fig. 7). An origin solely from rainfall, without the influence of sapping of subsurface liquids, is unlikely since this process would result in dendritic and branching morphologies with high stream orders, which is not observed borne out by the present image database. On the other hand, even on Earth and Mars it is currently still controversial whether sapping alone, without a contribution from rainfall and flood events, is able to cause these comparatively deep negative reliefs, especially in resistant rock (Lamb et al., 2006, 2008).

The suggested sapping processes would require high amounts of liquids stored in a subsurface aquifer, as proposed by Stevenson (1992). However, the idea of a subsurface methane reservoir was adopted by Stofan et al. (2007) in the context of possible interactions between the lakes close to the north pole and that 'methanifer'. Thus, sapping of subsurface liquids is generally considered conceivable.

4.4. Valleys in mountains

Mountain chains on Titan are suggested to be subject to intense resurfacing, at least partly due to fluvial erosion (Radebaugh et al., 2007; Lunine et al., 2008a). In fact, some of Titan's mountain chains exhibit putative channels, most of them appear inactive, incipient, and short, with lengths of several tens of kilometers and widths below 3 km (see Fig. 9a and Table 4). An exception to this is western Xanadu, which is traced by extended dendritic valley networks, as discussed in Section 4.1. Valleys within individual mountain ridges have a bright/dark-pairing in radar-images and possess a rather simple geometry. The type of mountain valleys is at or even below the radar instrument's resolution limit and most of the channels must be regarded as uncertain fluvial features owing to their small size. Furthermore, most of them are too short to identify certain morphologic characteristics or even network geometries that would to some extent confirm their fluvial origin. The course of those channels is difficult to trace because of the low contrast to their surroundings. Supporting a possible fluvial origin, some of these putative valleys are sinuous in shape, sometimes with several interconnections. If the observed features are in fact fluvial channels, their location in mountainous terrain suggests a high degree of erosion due to steep slopes and high flow velocities.

An example of these possible mountain valleys occurs at 347°W, 54°N (see Fig. 9a). Here, a surface feature with a west-eastern orientation can be identified that is clearly detached and totally distinct from the adjacent terrain, especially regarding its surface structure. It appears to be an elevated ridge, dissected by numerous channels. Although several sinuous valley-like features can be traced, the course of every channel and the underlying network geometry are beyond the resolution of the image data. The longest valley at the eastern margin of the ridge has a length of 50 km and a width of up to 3 km (see Fig. 9a). Similar to the Himalaya Range Fig. 9b, which is a comparably young formation, a relatively resistant basement seems to suppress the effect of resurfacing through fluvial erosion. The putative channels show a dominant orientation from NNE to SSW. The ridge is surrounded by homogeneous plains, as can be inferred from the undifferentiated and radar-dark characteristics of that terrain. Most valleys end abruptly at the edges of that mountain chain; their lower reaches, receiving streams or lakes are not visible. Either this is due to high evaporation rates, resulting in vanishing of the valleys or the recipient is subsequently eroded or covered by another layer. Taking into account the smoothness of adjacent areas it can be assumed that the surrounding terrain is younger and possibly sedimentary in origin. Radebaugh et al. (2007) proposed blankets of fluvial deposits that constitute the diffuse plains surrounding many mountain chains.

Possibly, dissected mountains on Titan represent remnants of former mountainous terrains, which covered the surface of Titan continuously. In this case, these features bear witness to a former wetter climate, strong tectonic processes and/or sedimentation. This assumption is supported by the fact that only the upper reaches of the valleys are visible, and candidate recipients are covered by sedimentary layers. On the other hand, the orientation and shape of mountain ridges is suggestive of a tectonic origin (Radebaugh et al., 2007), which argues against the theory of a divergence of a candidate primordial surface unit. The processes that lead to the divergence into mountainous areas and lowlands and to sedimentation remain controversial.

Alternatively, fluvial features within mountain chains can be interpreted as an evidence of orographic rainfall (Lopes et al., 2010; Barth, 2010). Topographic obstacles force air masses to rise and cool, followed by condensation, and formation of clouds, which is a common process on Earth. However, this interpretation does not explain why the majority of the channels end abruptly at the edges of mountains.

A glacial origin of the features can be excluded due to Titan's environmental conditions (Lorenz and Lunine, 1996; Perron et al., 2006).

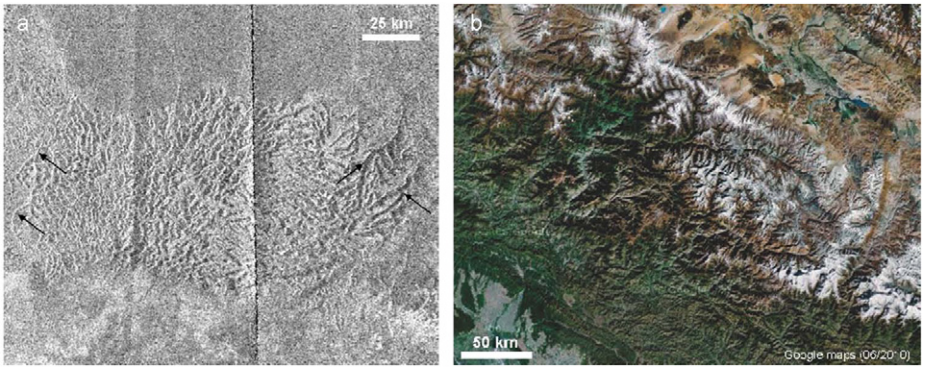

Fig. 9. a: mountain ridge with numerous potential channels. Radar-SAR T16 (July 22, 2006). Image is centered at 347°W, 54°N. Putative fluvial features are marked by arrows. b: mountain chain on Earth (Himalaya, northern Nepal). Image is centered at 29.39°N, 82.54°E (true color).

While the origin of mountain chains on Titan is still debated, it is very likely that mountains on Titan are composed of bedrock material whose resistance against erosion differs from that of the lowlands, and whose geologic age is most likely older (Stofan et al., 2006; Jaumann et al., 2009; Lopes et al., 2010).

4.5. Individual (elongated) valleys

Another type of valleys is to be found in regions that appear diffuse and homogeneous in radar-images, labeled as undifferentiated plains by Stofan et al. (2006) and Lopes et al. (2010). Valleys within plains appear bright in radar images, with a strong contrast to their radar-dark, featureless surroundings (see Fig. 10). This type of valleys differs from other valley types by its straight course with only few branches. Sinuous reaches, meanders and braiding features rarely occur, and the channel bends are of an angular rather than sinuous shape. Due to the incomplete coverage of the radar mapper, the source and mouth of the channels are not imaged and the course of these valleys is often fragmentary. Deltas or terminal deposits are also not recognizable in combination with this type of valleys. Owing to the low number of branches, the flow direction cannot be determined in most of the cases.

Valleys of this type emerge at all latitudes of Titan, except for the poles. Their global distribution is scattered and confined to the radar-dark featureless plains which, in turn, are uniformly distributed (Lopes et al., 2010). Valleys of this type are not wider than 3 km with lengths well below 100 km (see Table 4), although their lengths may in some cases be underestimated due to a fragmentary morphology.

The morphological characteristics of these putative valleys are in general indicative of a steady transport of liquids downstream, due to the valleys being of nearly constant width. If these features do, in fact, represent valleys due to fluvial flow, the delivery of liquids and the ambient conditions within undifferentiated terrains have been conceivably constant at the time of their formation. However, the radar-bright tone of the channels points to dry current climatic conditions. The simple shape and the absence of typical fluvial characteristics, such as meanders, suggest that these valleys were active for a shorter period of time than the other types of fluvial valleys on Titan because complex hierarchical geometries of channels with meanders and curvilinear shapes require a substantially longer time to develop (Ahnert, 2003).

A volcanic origin is also conceivable from a morphological point of view, given the predominantly constant width of the channels and the lack of integrated tributaries; attributes that are also typical for sinuous rilles on Venus and (Earth's) Moon (see Komatsu and Baker, 1996; Komatsu, 2007 and references herein). If this applies, the high radar backscatter of the channels would signify a rough surface of the solidified cryolava. While still under debate, there are several putative cryovolcanic domes and associated landforms, such as lava flows, calderas etc. (cf. Lopes et al., 2010; Le Corre et al., 2009; Jaumann et al., 2009), which underlines the significance of volcanic processes. On the other hand, lava flows on Titan show a laminar rather than linear flow as can be seen in Fig. 10 which argues against an origin from volcanic action of the linear channels shown here. An alternative development from rainfall is conceivable but cannot be verified because the source regions of these channels are not resolved. Seepage erosion is certainly not involved in the formation of these features given the narrow widths of the features and the lack of morphological indications for this process.

5. Spectral properties of fluvial terrain

VIMS-data reveal the subdivision of Titan's surface into bright, dark brown, and dark blue units (Porco et al., 2005; Barnes et al., 2007a; Soderblom et al., 2007a; Le Mouélic et al., 2008; Jaumann et al., 2008, 2009; Stephan et al., 2009), visibly obvious in false color composites of spectral bands within Titan's atmospheric windows with the following specifications: R: 1.58/1.28 μm, G: 2.0/1.28 μm, and B: 1.28/1.08 μm. Bright units are arranged in the form of 'islands' and large continents, such as Xanadu, Titan's largest continuous continent, centered at its leading hemisphere. Bright surfaces are interpreted to be older and elevated in contrast to dark 'nominal' surfaces (Griffith et al., 1991; Smith et al., 1996; Barnes et al., 2007a; Soderblom et al., 2007a; Jaumann et al., 2009). The bright unit is characterized by its high albedo in the atmospheric windows at short wavelengths, especially at 2 μm as well as in the utilized ratio composite. Bright continents and islands are interrupted by brown surfaces that broadly correlate with Titan's equatorial dune fields (Lorenz et al., 2006; Barnes et al., 2007a). Reflectance of the brown unit is comparatively low in all atmospheric windows (Barnes et al., 2007a) entailing a dark brown tone in the false color composite. The third spectral unit appears blue in the utilized ratio composite and often occurs at the eastern boundaries of bright terrains. This unit has a low reflectance at longer wavelengths (≥ 1.6 μm), and an increased reflectance at shorter wavelengths (≤ 1.3 μm) (Barnes et al., 2007a), resulting in an increased ratio value in the blue channel of the ratio composite. The blue material probably

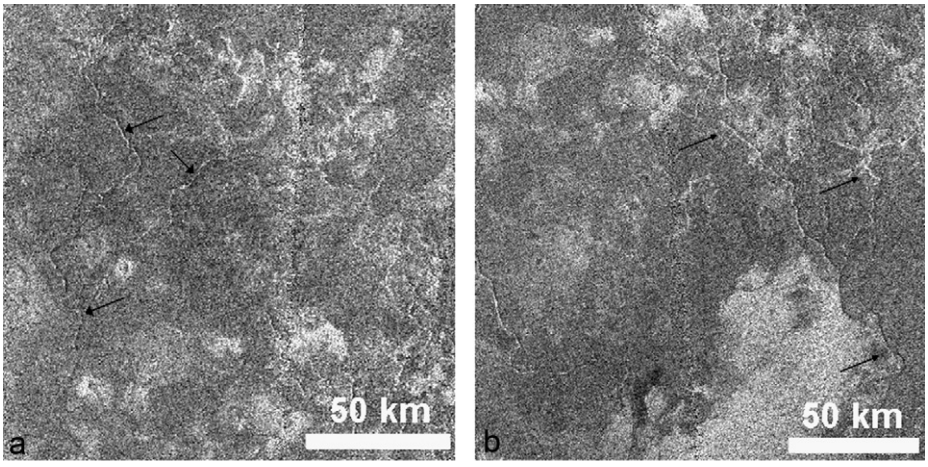

Fig. 10. Elongated valleys. a: radar-SAR T7 (September 07, 2005). Image is centered at 12°W, 56°S. b: radar-SAR T7 (September 07, 2005). Image is centered at 6°W, 58°S. Arrows indicate putative fluvial valleys.

has a higher water ice content compared to the other surface units, even though the entire spectral footprint has not been fully explained so far (Rodriguez et al., 2006; Soderblom et al., 2007a; Barnes et al., 2007b; Jaumann et al., 2008). Further information about the spatial and spectral attributes of the different surface types are given in Porco et al. (2005), Barnes et al. (2007a), Soderblom et al. (2007a), and Jaumann et al. (2008, 2009).

Fig. 11 shows the distribution of spectral surface units at Titan's lower latitudes according to VIMS-observations, overlayed with the database of fluvial valleys. Since the overlap between these data layers comprises only those areas between 30°N and 30°S (and here only those areas effectively covered by SAR, amounting to about 20% of the total surface of Titan), the results are not necessarily representative of the entire surface. However, the percentages indicate a strong tendency for the fluvial channels to be situated on the bright surfaces, visible in near-infrared images (see Table 3): Bright continents and islands host 84.4% of the valleys (percentage of the total channel length normalized by the area covered by the bright material). Only 3.5% of valleys emerge on the dark brown unit, and 12.1% out of the normalized valley-km at low latitudes relate to the dark blue surface unit. The small fraction of valleys outside bright terrains can result from a spatial mismatch between VIMS and SAR data due to the spatial resolution of VIMS being some orders coarser than the radar-resolution. In VIMS images with a resolution of 10 km/pixel, boundaries between different spectral units can be blurred (mixed-pixel effect), and channels situated near that boundary are assigned to the spectral unit that takes up the larger part of the pixel. Nevertheless, the majority of valleys are located too far from these transitions, or at least several VIMS pixels away from the boundary of spectral units, so that the influence of mixed pixels is clearly of minor significance. Despite this, at least one possible channel cutting through dunes is mentioned in a publication by Barnes et al. (2008). But, although dark blue and brown surfaces together account for almost 40% of the surface near the equator, only about 15% of the valleys are situated here.

Through spectral investigations of high-resolution VIMS observations combined with SAR-images, Barnes et al. (2007b) discovered a spectral analogy between the material covering fluvial channels situated at Titan's low latitudes and the dark blue surface unit. Both, images obtained with VIMS and radar resolved fluvial channels several hundreds of kilometers long and up to 2 km wide. Fig. 5 in Barnes et al. (2007b) depicts a valley that is visible through a series of VIMS pixels with a bluish spectral footprint. Remarkably, the estimated width of the valley (0.8–1.0 km, based on the radar observation) is significantly smaller than the VIMS resolution at that location (between 4.5 and 6.6 km per pixel) (Barnes et al., 2007b). Jaumann et al. (2008) confirmed this connection between fluvial features and the bluish surface unit through spectral investigations of fluvial features in other regions, such as Chusuk Planitia. In this case, channels drain into what could be a former receiving sea or bay that is covered by dark blue sediments. An important implication of that observation is that the blue material possibly represents layers of fluvial debris, systematically sedimented due to a decreasing flow velocity when reaching the receiving stream (Jaumann et al., 2008). This correlation is confirmed at the HLS, where fluvial channels drain into a putative lake characterized by similar spectral properties, i.e. showing the spectral footprint of the bluish material (Rodriguez et al., 2006).

Considering the high relevance of fluvial incision on Titan obvious from the high number and great areal coverage of its valleys, it seems reasonable to assume that fluvial sediments should also cover large areal fractions of the surface, possibly those 7% of the surface covered by the dark blue surface units at lower latitudes. However, a direct correlation between the dark blue unit and Titan's valleys is not detected by an investigation on this large scale. While extensive VIMS-blue terrains occur around Titan's equator, channels are few in numbers. It may be expected with a high level of certainty that many other valleys exist, which are too narrow and too short to be resolved by VIMS or radar. With increasing spatial resolution, such as at the HLS and at Chusuk Planitia, very distinct channels appear, emerging from the bright areas and draining into the blue terrains. Furthermore, the coverage by image data of the various sensors is still far from complete what reduces the reliability of this statistical approach. Although the absence of channels around the blue surface unit can be due to insufficient resolution or coverage, the fact that channels are closely associated with bright surfaces seem to preclude the assumption of fluvial deposition causing the accumulation of dark blue sediments. Besides, only 7% of the valleys at low latitudes (between $\pm 30^{\circ}$) are located less than 100 km away

Table 3
Allocation of channels on the spectral units.

Spectral unit	Number of channels (percent of the total number)	Lengths of the channel (percent of the total channel length)	Percentage of the total channel length (normalized by the surface area)
Bright spectral unit	341 (93.94)	12,071.32 km (96.2)	84.4
Blue spectral unit	7 (1.93)	201.48 km (1.6)	12.1
Brown spectral unit	14 (3.86)	269.67 km (2.2)	3.5

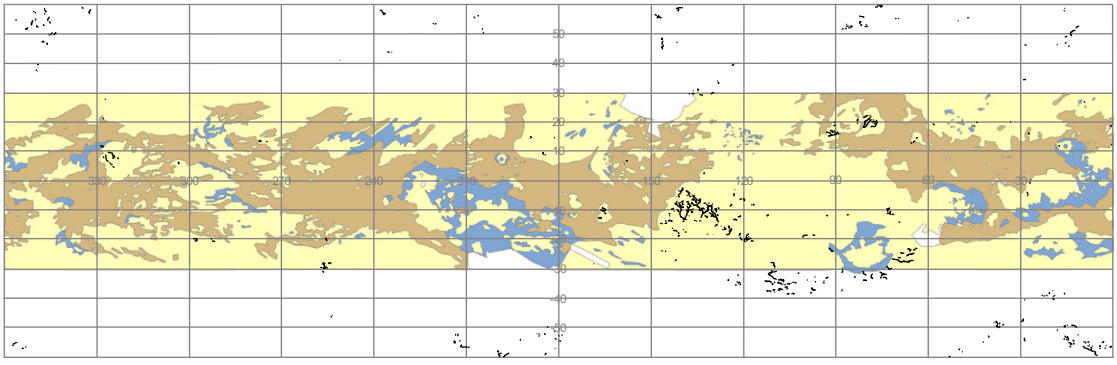

Fig. 11. Map of spectral units on Titan with the same coloring as introduced in the text. Fluvial valleys are marked in black. Simple cylindrical projection of Titan's lower and mid-latitudes.

from the blue surface unit as shown in Fig. 13 (or nearly 10% based on valley length).

Nevertheless, it is noticeable that bright surfaces are dissected by numerous streaks or basins of bright-bluish color. In fact, the bright surface unit is spectrally the least homogeneous unit, and exhibits substantial albedo differences. Moreover, high-resolution VIMS data of fluvial terrain possess spectral properties intermediate between the dark blue and the bright spectral signature (Barnes et al., 2007b; Langhans et al., 2010). Fig. 12 shows ratio-spectra of fluvial terrains extracted at western Xanadu. Spectra of the bright and the blue surface units were added for comparison. Pixels in the vicinity of fluvial features behave as a mixture of bright and blue surfaces in spectral terms.

This observation suggests that dark blue areas or streaks are integrated within the bright continents; these are too small to be detected and cause mixed pixels within the bright unit. Bright materials have a higher spatial fraction at the pixel, resulting in an assignment to the bright surface unit. Again, high-resolution data of the HLS (overlayed with DISR-images) as well as of Chusuk Planitia support the assumption of channels draining from bright highlands into dark blue lowlands where sedimentation conceivably causes the blue spectral characteristics of the uppermost surface layer (Jaumann et al., 2008).

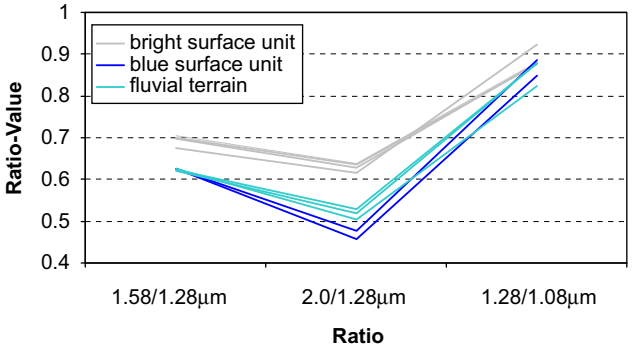

Fig. 12. Ratio-spectra of fluvial terrain, bright, and blue surface units (R: 1.58/1.28 μm, G: 2.0/1.28 μm, and B: 1.28/1.08 μm). Western Xanadu. Valleys are identified and traced by means of radar data (T13, April 30, 06). VIMS-data (observation T12, March 18, 2006, max. resolution of 7 km/pixel) were overlayed and spectra were extracted at VIMS pixels dissected by fluvial features. Spectra of pure blue and bright pixels are added for comparison. VIMS pixel are considerably larger than the estimated width of the valleys. Nevertheless, the fluvial terrain exhibits intermediate spectral properties lying between those of bright and blue surfaces. (For interpretation of the references to color in this figure legend, the reader is referred to the web version of this article.)

6. Distribution

Despite their widespread distribution over all latitudes on Titan (see Figs. 1, 11, 14, 15, and Table 4) fluvial valleys are not homogeneously distributed. A detailed view discloses centers of fluvial activity at some locations, while other areas are devoid of channels (see Fig. 15). If one divides the imaged areas into 225 km wide boxes (5° at the equator), only 20.5% of boxes of the total imaged area contain channels. Landscapes not influenced by fluvial erosion clearly prevail, while valleys are concentrated in comparatively small regions. The majority of channels are shorter than 50 km (see Fig. 15, right), irrespective of their particular location, while the largest channels are situated between 10°S and 40°S (associated to western Xanadu) and around 20°N (Elivagar Flumina channel system, located east of Menrva). Less surprisingly, areas with a relatively high channel density host the largest channels. These dense networks are located at western Xanadu (Barnes et al., 2007b; Lorenz et al., 2008), near the HLS (Tomasko et al., 2005) as well as close to the north pole (Stofan et al., 2007; Mitchell et al., 2007). In general, fluvial landforms seem to be associated with mountainous or rugged terrain as many of Titan's valleys emerge in radar-bright areas (Radebaugh et al., 2007; Lopes et al., 2010). Similarly, channels have been found in association with impact craters (Elachi et al., 2006; Lorenz et al., 2008; Soderblom et al., 2010). Thus, channels appear to be linked to regions with comparatively high slopes and substantial elevation differences. Long and sinuous valleys occur in the vicinity of the large north polar lakes ($>70°$N, 210−360°W) (Stofan et al., 2007; Mitchell et al., 2007). However, the north polar region is dichotomic regarding the distribution of fluvial features. Despite of many small lakes between 0 and 150°W at high northern latitudes, which are partly drained and liquid-filled (Stofan et al., 2007) valleys are sparse, short, and stubby in that region (see Fig. 14), more consistent with processes due to interaction with a subsurface methane table (Stofan et al., 2007).

Only a small number of valleys with simple network geometries appear near the south pole (see Fig. 14) and on undifferentiated plains, at mid-latitudes. Nevertheless, some valleys emerge at the featureless dark plains, which in turn are interpreted to be sedimentary in origin by Lopes et al. (2010). Nearly no valleys occur within flat dunefields that cover almost one third of the surface at low latitudes. Only one possible channel, situated within the dunefields, has been found so far (Barnes et al., 2008). Fluvial and aeolian erosion are competing in the sense that each of these processes – if dominating over a substantial time – tend to substitute or even out the landforms created by the other process. Several scenarios explain the

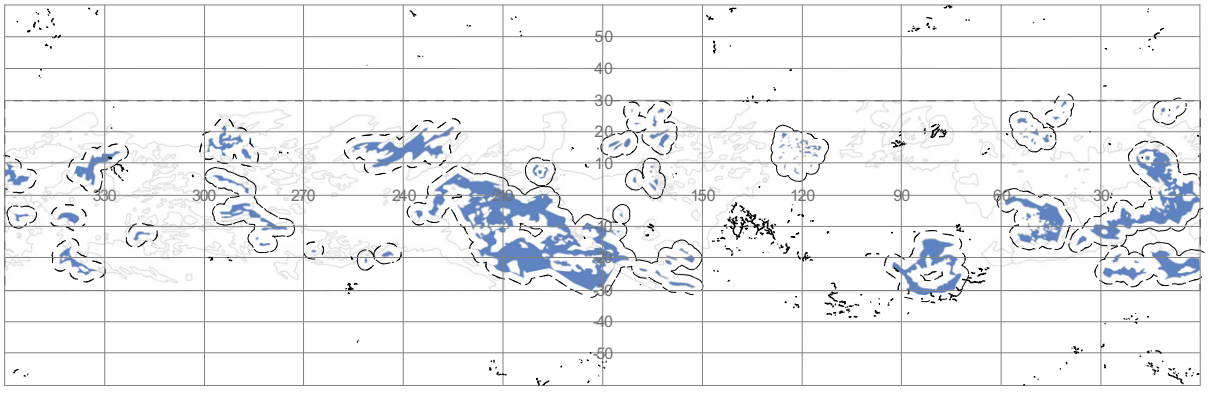

Fig. 13. Global map of Titan's low and mid-latitudes, simple cylindrical projection. Blue spectral unit is marked in light blue. Buffer around the blue unit (100 km) is indicated by dashed lines. Fluvial valleys are marked in black.

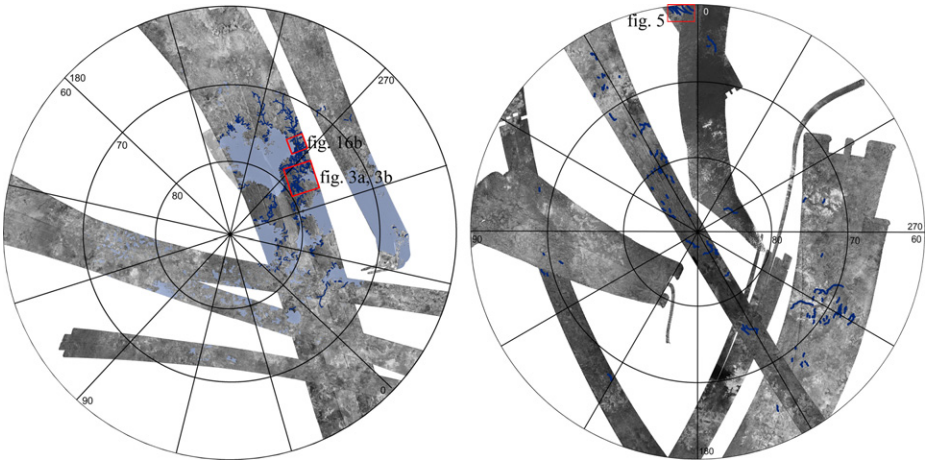

Fig. 14. Circular maps of Titan's polar regions, generated from radar swaths. Left: north polar region. Valleys and lakes are superimposed. Right: south polar area, fluvial valleys highlighted in blue.

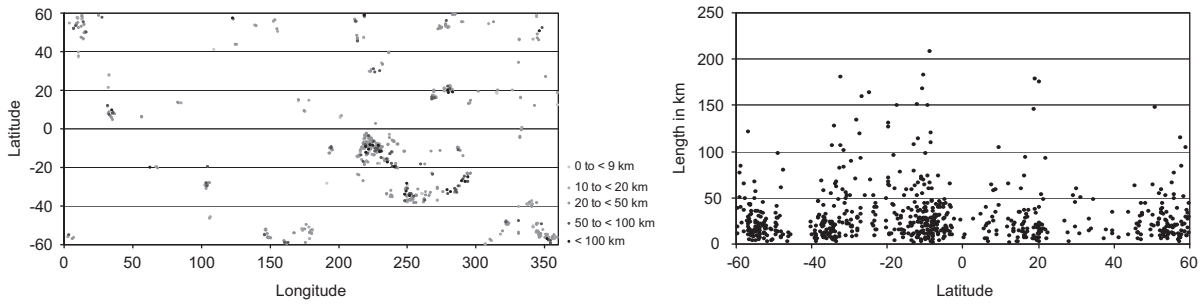

Fig. 15. Left: scatterplot of geographic position of fluvial valleys on Titan. Lengths of the valleys are indicated in levels of gray. Right: scatterplot of channel-length vs. latitude.

absence of fluvial features in Titan's dunefields: It is expected that the youngest processes taking place on Titan are the accumulation of dunes and the incision of channels (Barnes et al., 2008; Lopes et al., 2010). Possibly, the accumulation of dunes took place subsequent to the incision of channels and maybe even proceeds today so that dune-layers might, in fact, be covering subjacent valleys (Barnes et al., 2008; Lopes et al., 2010). An alternative assumption would be that fluvial erosion is not equally distributed, with rainfall being restricted to certain areas, analogous to the situation on Earth. Supporting this, the formation of dunes requires dry and desert-like conditions which generally argues against a simultaneous development of channels. On the other hand, the distribution of valleys is correlated to the presence of mountains, which can be an indication for orographic rainfall (Lopes et al., 2010) and a deficit of precipitation in the plains. Another explanation for the apparent absence of fluvial valleys within the dunefields is that valleys are present but too small and narrow to be resolved by radar. This explanation is unlikely since larger channels are resolved at all latitudes on Titan and the complex distribution of channels is certainly due to the climatic and/or geologic reasons described above.

Titan's valleys have enormous dimensions, with lengths up to several hundreds of kilometers (see Table 4). Dendritic valleys have the highest lateral extensions. The average length of all valleys imaged until T57 (June 2009) is 30 km, but this value is certainly underestimated due to the incomplete coverage and the segmented storage of valleys in the database. In most of the cases, the width of the valleys does not exceed several pixels, sometimes with unknown fractions hidden by radar-shadow (see Fig. 16A). Most of the broader, north-polar valleys assumed to have been active recently have widths of 1–2 km (see Fig. 16B). Some of the valleys (labeled as 'dry valleys' here) reach widths of several kilometers (10 km in T3, Fig. 16C; up to 8 km in T44, Fig. 16D, see Table 4). Thus, valleys on Titan are comparable to major terrestrial and Martian channels in their geometric dimensions (Jaumann et al., 2010).

High latitudes, both in the north polar as well as in the south polar regions, exhibit fluvial valleys (see Fig. 14). However, the valley (and lake) density is higher around the north pole and, most importantly, north polar valleys are currently active (Stofan et al., 2007; Wye et al., 2009; Stephan et al., 2010), a fact also confirmed by cloud observations at these latitudes by Brown et al. (2009). On the other hand, clouds have also been observed near the south pole, which weakens the argument of a pronounced seasonality (Rodriguez et al., 2009; Brown et al., 2010). Yet, so far only few, smaller and eroded lakes have been found close to the south pole (Lunine et al., 2008b); several, probably active, channels discharge into the largest lake—Ontario Lacus (Wall et al., 2010). Additionally, spectral observations suggest a shrinking of the southern Ontario Lacus (Barnes et al., 2009a; Turtle et al., in press; Hayes et al., 2011). Supporting that observation, only few channels emerge in this region (see Fig. 14), and most of them are empty. The distribution of dry versus filled channels in the polar regions mirrors the state of the lakes. These observations support the findings in Stofan et al. (2007) and Lunine et al. (2008b) who suggested that a transport of moisture in the atmosphere is taking place between the two hemispheres. This process is possibly a seasonal effect, since evaporation is attributed to the summer hemisphere while rainfall is suggested to take place in the winter hemisphere

Table 4
Database of fluvial network systems on Titan.

Longitude	Latitude	Dataset	Date	Type	Length	Width	Stream Order	References
High southern latitudes		ISS T0	July 2, 2004	Dendritic	> 1000 km	10–20 km	2nd	Fig. 2 in Porco et al. (2005)
80°W	54°N	Radar TA	October 26, 2004	Fan-like, delta	Several tens of km	0.5–1 km	1st	Fig. 2 in Lorenz et al. (2008), Paganelli et al. (2005)
192°W	10.6°S	DISR	January 14, 2005	Dendritic	< 15 km	< 250 m	4th	e.g. Fig. 5 in Tomasko et al. (2005), Fig. 1 in Perron et al. (2006), Figs. 8 and 9 in Soderblom et al. (2007b), Fig. 4 in Jaumann et al. (2008), Fig. 4 this work
192°W	10.6°S	DISR	January 14, 2005	Sapping	< 10 km	Some tens of meters	2nd to 3rd	Fig. 5 in Tomasko et al. (2005), Fig. 8 in Soderblom et al. (2007b), Fig. 7 this work
77°W	19°N	Radar T3	February 15, 2005	Dry	10–200 km	< 10 km	2nd to 3rd	Fig. 3 in Lorenz et al. (2008), Fig. 5c in Stofan et al. (2006), Fig. 16c this work
90°W	16°N	Radar T3	February 15, 2005	Dendritic	< 200 km	< 3 km	2nd to 3rd	Fig. 3 in Lorenz et al. (2008), Fig. 4 in Burr et al. (2009)
7°W	59°S	Radar T7	September 2007, 05	Dry	< 150 km	1–2 km	Braiding	Fig. 6 in Lorenz et al. (2008), Fig. 4 in Burr et al. (2009), Fig. 5 this work
12°W	56°S	Radar T7	September 07, 2005	Elongated	< 100 km	< 3 km	2nd	Fig. 5 in Lorenz et al. (2008), Fig. 10a this work
6°W	58°S	Radar T7	September 07, 2005	Elongated	< 100 km	< 3 km	2nd to 3rd	Fig. 5 in Lorenz et al. (2008), Fig. 10b this work
138°W	10°S	Radar T13, Radar T44	April 30, 2006, May 28, 2008	Dendritic	< 450 km	300 m to 2.5 km	6th to 7th	Fig. 7 in Lorenz et al. (2008), Figs. 1 and 2 in Burr et al. (2009), Fig. 3c and d this work
125°W	10°S	VIMS TB, Radar T13	December 13, 2004, April 30, 2006	Dendritic	< 300 km	800 m to 1 km	2nd to 3rd	Fig. 5 in Barnes et al. (2007b)
66°W	10°S	VIMS T9, Radar T13	December 26, 2005, April 30, 2006	Elongated	50–100 km	800–2000 m	1st	Figs. 3 and 4 in Barnes et al. (2007b)
50°W	12°S	VIMS T9	December 26, 2005	Dendritic	100–200 km	800–2000 m	2nd to 3rd	Fig. 2 in Barnes et al. (2007b)
140°W	8°S	Radar T13	April 30, 2006	Dendritic	140 km	350–1400 m	2nd	Fig. 2 in Jaumann et al. (2008)
347°W	54°N	Radar T16	July 22, 2006	Mountain valley	< 70 km	< 3 km	2nd	Fig. 9a this work
143°W	50°N	Radar T16	July 22, 2006	Sapping	~ 200 km	< 5 km	2nd	Fig. 8 this work
345°W	75°N	Radar T19, Radar T25	October 2009, 2006; February 22, 2007	Dendritic	~ 100 km	500–1000 m	2nd to 3rd	Fig. 8 in Lorenz et al. (2008)
255°W	75°N	Radar T28	April 10, 2007	Dendritic	1200 km	1400–3000 m	4th to 5th	Fig. 2 in Jaumann et al. (2008), Fig. 16b this work
280°W	78°N	Radar T28	April 10, 2007	Dendritic	< 200 km	300 m to 5 km	4th to 5th	Fig. 3a and b this work
67°W	27°S	Radar T41	February 22, 2008	Dry	~ 350 km	< 3 km	2nd	Fig. 6 this work
107°W	36°S	Radar T41	February 22, 2008	Mountain valley	Some tens of km	< 1 km	1st	Fig. 16a this work
120°W	17°S	Radar T44	May 28, 2008	Dry	< 180 km	1–8 km	1st	Fig. 1b in Le Gall et al. (2010), Fig. 16d this work
185°W	72°S	Radar T49, Radar T57 Radar T58	December 21, 2008 June 22, 2009 July 08, 2009	Flooded channel, estuary	Several tens of km	1–3 km	1st	Fig. 1 in Wall et al. (2010)

(Rannou et al., 2006; Stofan et al., 2007). Currently, the southern hemisphere switches from summer into autumn (Lorenz et al., 2009) and a reversing of climatic conditions is expected (Stevenson and Potter, 1986; Stofan et al., 2007; Lunine et al., 2008b). Alternatively, the observed unequal distribution of filled and abandoned lakes and channels might be the result of Saturn's eccentricity that leads to differences in precipitation and evaporation between Titan's hemispheres (Aharonson et al., 2009). In addition, recent studies report on increased summer precipitation at high latitudes based on models of Titan's atmosphere and circulation (Tokano, 2009; Mitchell et al., 2009). These models are not consistent with the observations of fluvial features in the present paper. To prove any seasonal variations in rainfall, the rate and variation of precipitation and evaporation have to be significant. Otherwise the distinctly unequal distribution of active and abandoned lakes and channels is more likely to be a regional or orographic phenomenon.

Generally, the global ubiquity of valleys is not consistent with the recent scarcity of tropospheric clouds and their confinement to certain latitudes within the last six years of Cassini-observation (see Lorenz et al., 2005; Brown et al., 2010 and references herein). Together with the fact that the majority of channels is most likely empty today, this suggests that the past climate state was more humid than the dry situation today, or that rainfall and fluvial

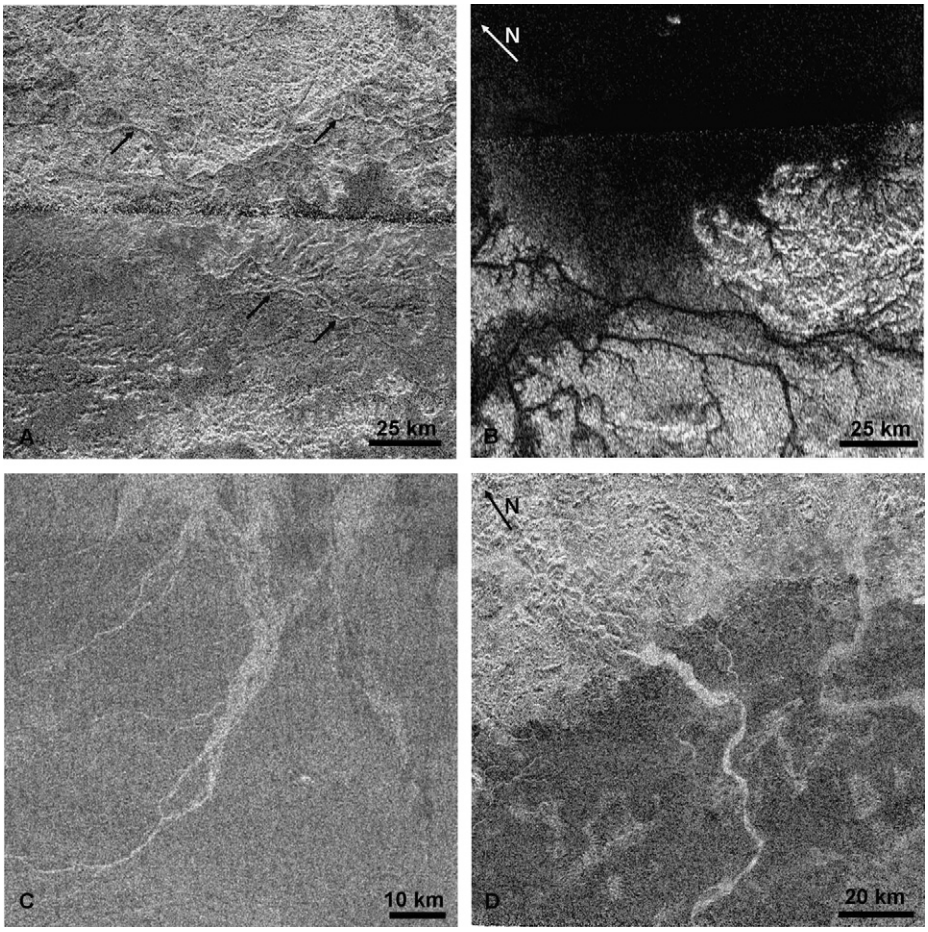

Fig. 16. Geometric dimensions of fluvial valleys on Titan. (A) Fluvial valleys south of Xanadu (radar T41, February 22, 2008). Image is centered at 36°S, 107°W. Radar shadows highlighted by the arrows (illumination from south). (B) Fluvial valleys near the north pole (radar T28, April 10, 2007). Image is centered at 76°N, 263°W. (C) Dry fluvial valleys east of Menrva crater (radar T3, February 15, 2005). Image is centered at 19°N, 77°W. (D) Fluvial valleys south of Xanadu (radar T44, May 28, 2008). Image is centered at 17°S, 125°W.

incision are ephemeral phenomena in space and time. Supporting this, many valleys show a morphologic resemblance to dry valleys and wadis on Earth (see Section 4.2). It is conceivable that in recent times, Titan has seen episodic individual violent storm events, which would explain the many fluvial landscapes found on its surface. Similarly, terrestrial deserts have developed prominent fluvial features despite low mean rainfall rates.

Another clue provided by the global distribution of valleys is given through their close association with mountains (Radebaugh et al., 2007) and their conceivable orographic origin (Lopes et al., 2010; Barth, 2010). Although elevation differences are in the order of several hundreds of meters, with peak heights not exceeding 2 km, the correlation between these landforms is apparent. Alternative explanations for the correlation between rugged terrains and channels are that mountainous terrain is less resistant to fluvial incision, or that mountains, as opposed to plains and dunefields are not subject to sedimentation. Unfortunately, these hypotheses cannot be verified at the current image resolution and coverage.

Generally, Titan's valleys seem young on geologic timescales due their pristine and undegraded morphology (Soderblom et al., 2007b; Lunine and Atreya, 2008). When comparing different types of fluvial valleys regarding their relative age, dendritic valleys appear to be the oldest systems because their physiography can only be explained by a steady flow over a certain period of time. Other valleys that can be considered among the oldest channels are valleys in mountains. The often fragmentary course of these valleys possibly indicates degradation, through mechanical erosion or impact cratering, while it could also be a resolution effect. The other end of the scale – the youngest fluvial features – is difficult to assess since the absolute date of origin of fluvial features cannot be determined. Sinuous, linear landforms due to fluvial flow can develop in a comparably short time (minutes to hours) and relict valleys can, in the absence of other erosional processes, remain at the surface for substantial time. It would be a misconception to denote the active northern valleys as the youngest features owing to recent rainfall. It is equally possible for the entire north polar fluvial system to be relatively old and active on seasonal timescales.

It is difficult to explain the distribution of channels from recent cloud observations. Dendritic valleys are located in high and low latitudes, while the mid-latitudes are dominated by dry channels. Candidate sapping channels emerge only at two locations (at the HLS and at mid-latitudes) while lakes considered to be connected to a subsurface methane table are confined to high northern latitudes (Hayes et al., 2008). The distribution of mountain valleys is restricted to rugged, radar-bright terrains, which in turn are scattered around Titan's lower latitudes (mainly between $\pm 30^{\circ}$ (Radebaugh et al., 2007; Lopes et al., 2010)) and seem to be more affected by orographic processes than by the global circulation. Individual elongated valleys are scattered over all latitudes of Titan with the exception of the polar areas. As in most of the other types of valleys, these features are indicative of previous rainfall, possibly a wetter climate in the past and a

predominantly dry climate today (Griffith et al., 2008; Lunine and Lorenz, 2009).

On a global scale several particularities make Titan's valleys differ from those of terrestrial rivers: Fluvial transport of some candidate channels takes place over several hundreds of kilometers, sometimes without any convergence with other tributaries and without any morphologic changes in flow. Also, many putative fluvial channels seem to vanish without a previous thinning out of the interior channel, pointing to an abrupt change of the boundary conditions either in the catchment or at the vanishing point, although a volcanic origin of the flows is also conceivable (see Section 4.5). Many of the observed fluvial features do not drain into a receiving lake or sea, as they would on Earth, although a number of terminal lakes are observed close to the north pole (Stofan et al., 2007), at the HLS (Tomasko et al., 2005; Soderblom et al., 2007b), and in the Chusuk Planitia region (Jaumann et al., 2008).

Except for the high northern latitudes where recent rainfall is very likely, Titan's climate appears to be predominantly arid, at least in recent times (Lorenz and Lunine, 1996; Lorenz, 2000; Lorenz et al., 2008; Lunine and Lorenz, 2009). The fact that fluvial erosion is not restricted to certain latitudes and that at least the abandoned fluvial valleys occur virtually at all latitudes, underlines that Titan's surface has previously experienced rainfall globally.

7. Conclusions

Studied in a global context, Titan's valleys reveal some very diverse properties and geological features, both in a spectral and in a morphological sense. The high morphological diversity of Titan's valleys presumably arises from a variety of processes causing and affecting fluvial erosion, such as sapping through subsurface liquids, precipitation, the influence of different rainfall regimes, different substrate types or varying resistance against erosion of the bedrock material. These highly variable conditions, both in space and time, have led to complex landforms.

Fluvial valleys show a great morphologic diversity, with many of them resembling terrestrial valley types. The most prominent fluvial type is the dendritic. Although fluvial valleys can be found at all latitudes on Titan, some regions show dense networks of valleys while others are channel-free. Extensive dendritic valley networks can be found at Titan's equator and near the north pole. For the latter, recent precipitation is the most likely explanation. This region is the only exception in a predominantly dry climatic situation, as can be inferred from the high radar return of the majority of Titan's valleys. From the global valley distribution and their particular radar return it can be concluded that the equatorial areas – especially the dunefields – are currently as dry as desert regions on Earth. Many morphologic indications suggest an episodic character and an ephemeral nature of the methane cycle within these latitudes.

Spectrally, Titan's fluvial valleys are associated with the bright surface unit. Only very few valleys are to be seen on the VIMS-brown unit, although this could be caused by the VIMS resolution being insufficient, or by a spatial mismatch between VIMS and radar-SAR. The assumption that the blue material corresponds to fluvial deposits could neither be confirmed nor shown to be false. However, what supports this idea is the presence of some examples where the assumed conditions are met as well as the fact that a certain number of valleys are situated close to the blue spectral unit. Furthermore, spectral investigations of individual valleys reveal that the spectral footprint of fluvial terrains is often a mixture between the bright and the blue spectral signature. Although many questions concerning the global distribution and characteristics of fluvial erosion on Titan have been addressed, some issues still remain controversial and must await future investigations based on higher-resolution data.

Acknowledgements

We thank the Cassini-RADAR team for providing the RADAR-SAR database utilized in this paper. We gratefully acknowledge the work done by the Cassini VIMS team that made our spectral analysis possible. This work was greatly improved from written feedback provided by two anonymous reviewers. This research has been carried out at the DLR Institute of Planetary Research with support by the Helmholtz Association as part of the research alliance 'Planetary Evolution and Life'.

References

Aharonson, O., Hayes, A.G., Lunine, J.I., Lorenz, R.D., Allison, M.D., Elachi, C., 2009. An asymmetric distribution of lakes on Titan as a possible consequence of orbital forcing. Nature Geoscience 2, 851–854.

Ahnert, F., 2003. Einfuehrung in die Geomorphologie. Verlag Eugen Ulmer Stuttgart.

Atreya, S.K., Adams, E.Y., Niemann, H.B., Demick-Montelara, J.E., Owen, T.C., Fulchignoni, M., Ferri, F., Wilson, E.H., 2006. Titan's methane cycle. Planetary and Space Science 54, 1177–1187.

Atreya, S.K., Lorenz, R.D., Waite, J.H., 2009. Volatile origin and cycles: nitrogen and methane. In: Brown, R.H., Lebreton, J.-P., Waite, J.H. (Eds.), Titan from Cassini-Huygens. Springer.

Baker, V.R., 2001. Water and the martian landscape. Nature 412 (July), 228–236.

Baker, V.R., Kochel, R.C., Laity, J.E., Howard, A.D., 1990. Spring sapping and valley network development. In: Higgins, C.G., Coates, D.R. (Eds.), Groundwater geomorphology: the role of subsurface water in earth-surface processes and landforms. Geological Society of America Special Paper, Boulder, Colorado, pp. 235–265.

Barnes, J.W., Brown, R.H., Soderblom, J.M., Soderblom, L.A., Jaumann, R., Jackson, B., Le Mouélic, S., Sotin, C., Buratti, B.J., Pitman, K.M., Baines, K.H., Clark, R.N., Nicholson, P.D., Turtle, E.P., Perry, J., 2009a. Shoreline features of Titan's Ontario Lacus from Cassini/VIMS observations. Icarus 201 (May), 217–225.

Barnes, J.W., Brown, R.H., Soderblom, L., Buratti, B.J., Sotin, C., Rodriguez, S., Le Mouélic, S., Baines, K.H., Baines, K.H., Clark, R., Nicholson, P.D., 2007a. Global-scale surface spectral variations on Titan seen from Cassini/VIMS. Icarus 186, 242–258.

Barnes, J.W., Brown, R.H., Soderblom, L., Sotin, C., Le Mouèlic, S., Rodriguez, S., Jaumann, R., Beyer, R.A., Buratti, B.J., Pitman, K., Baines, K.H., Clark, R., Nicholson, P., 2008. Spectroscopy, morphometry, and photoclinometry of Titan's dunefields from Cassini. Icarus 195, 400–414. URL: 〈http://wwwsciencedirect.com/science/article/B6WGF-4RH380F-2/2/9ab3fc3eebb61da51a8a900f61a5033c〉.

Barnes, J.W., Radebaugh, J., Brown, R.H., Wall, S., Soderblom, L., Lunine, J., Burr, D., Sotin, C., Le Mouélic, S., Rodriguez, S., Buratti, B.J., Clark, R., Baines, K.H., Jaumann, R., Nicholson, P.D., Kirk, R.L., Lopes, R., Lorenz, R.D., Mitchell, K., Wood, C.A., 2007b. Near-infrared spectral mapping of Titan's mountains and channels. Journal of Geophysical Research (Planets) 112, 11006.

Barnes, J.W., Soderblom, J.M., Brown, R.H., Buratti, B.J., Sotin, C., Baines, K.H., Clark, R.N., Jaumann, R., McCord, T.B., Nelson, R., Le Mouélic, S., Rodriguez, S., Griffith, C., Penteado, P., Tosi, F., Pitman, K.M., Soderblom, L., Stephan, K., Hayne, P., Vixie, G., Bibring, J., Bellucci, G., Capaccioni, F., Cerroni, P., Coradini, A., Cruikshank, D.P., Drossart, P., Formisano, V., Langevin, Y., Matson, D.L., Nicholson, P.D., Sicardy, B., 2009b. VIMS spectral mapping observations of Titan during the Cassini prime mission. Planetary and Space Science 57, 1950–1962. URL: 〈http://wwwsciencedirect.com/science/article/B6V6T-4W7421G-3/2/1e05f0b0392c3df86b9e7562c0d7fa9a〉.

Barth, E.L., 2010. Cloud formation along mountain ridges on Titan. Planetary and Space Science 58, 1740–1747.

Brown, M.E., Roberts, J.E., Schaller, E.L., 2010. Clouds on Titan during the Cassini prime mission: a complete analysis of the VIMS data. Icarus 205, 571–580.

Brown, M.E., Schaller, E.L., Roe, H.G., Chen, C., Roberts, J., Brown, R.H., Baines, K.H., Clark, R.N., 2009. Discovery of lake-effect clouds on Titan. Journal of Geophysical Research 36, L01103.

Brown, R.H., Baines, K.H., Bellucci, G., Buratti, B.J., Capaccioni, F., Cerroni, P., Clark, R.N., Coradini, A., Cruikshank, D.P., Drossart, P., Formisano, V., Jaumann, R., Langevin, Y., Matson, D.L., McCord, T.B., Mennella, V., Nelson, R.M., Nicholson, P.D., Sicardy, B., Sotin, C., Baugh, N., Griffith, C.A., Hansen, G.B., Hibbitts, C.A., Momary, T.W., Showalter, M.R., 2006. Observations in the Saturn system during approach and orbital insertion, with Cassini's Visual and Infrared Mapping Spectrometer (VIMS). Astronomy & Astrophysics 446, 707–716.

Brown, R.H., Soderblom, L.A., Soderblom, J.M., Clark, R.N., Jaumann, R., Barnes, J.W., Sotin, C., Buratti, B., Baines, K.H., Nicholson, P.D., 2008. The identification of liquid ethane in Titan's Ontario Lacus. Nature 454, 607–610.

Burr, D.M., Emery, J.P., Lorenz, R.D., Collins, G.C., Carling, P.A., 2006. Sediment transport by liquid surficial flow: application to Titan. Icarus 181, 235–242.
Burr, D.M., Jacobsen, R.E., Roth, D.L., Phillips, C.B., Mitchell, K.L., Viola, D., 2009. Fluvial network analysis on Titan: evidence for subsurface structures and west-to-east wind flow, southwestern Xanadu. Geophysical Research Letters 36, 22203.
Butzer, K.W., 1976. Geomorphology from the Earth. Harper & Row, New York.
Clark, R.N., Curchin, J.M., Barnes, J.W., Jaumann, R., Soderblom, L., Cruikshank, D.P., Brown, R.H., Rodriguez, S., Lunine, J., Stephan, K., Hoefen, T.M., Le Mouèlic, S., Sotin, C., Baines, K.H., Buratti, B.J., Nicholson, P.D., 2010. Detection and mapping of hydrocarbon deposits on Titan. Journal of Geophysical Research (Planets) 115 (E14), 10005.
Collins, G.C., 2005. Relative rates of fluvial bedrock incision on Titan and Earth. Geophysical Research Letters 32, 22202.
Elachi, C., Allison, M.D., Borgarelli, L., Encrenaz, P., Im, E., Janssen, M.A., Johnson, W.T.K., Kirk, R.L., Lorenz, R.D., Lunine, J.I., Muhleman, D.O., Ostro, S.J., Picardi, G., Posa, F., Rapley, C.G., Roth, L.E., Seu, R., Soderblom, L.A., Vetrella, S., Wall, S.D., Wood, C.A., Zebker, H.A., 2004. Radar: the Cassini Titan radar mapper. Space Science Reviews 115, 71–110.
Elachi, C., Wall, S., Janssen, M., Stofan, E., Lopes, R., Kirk, R., Lorenz, R., Lunine, J., Paganelli, F., Soderblom, L., Wood, C., Wye, L., Zebker, H., Anderson, Y., Ostro, S., Allison, M., Boehmer, R., Callahan, P., Encrenaz, P., Flamini, E., Francescetti, G., Gim, Y., Hamilton, G., Hensley, S., Johnson, W., Kelleher, K., Muhleman, D., Picardi, G., Posa, F., Roth, L., Seu, R., Shaffer, S., Stiles, B., Vetrella, S., West, R., 2006. Titan Radar Mapper observations from Cassini's T3 fly-by. Nature 441, 709–713.
Flasar, F.M., 1983. Oceans on Titan? Science 221, 55–57.
Griffith, C.A., McKay, C.P., Ferri, F., 2008. Titan's tropical storms in an evolving atmosphere. The Astrophysical Journal 687, L41–L44.
Griffith, C.A., Owen, T., Wagener, R., 1991. Titan's surface and troposphere, investigated with ground-based, near-infrared observations. Icarus 93, 362–378.
Hayes, A., Aharonson, O., Callahan, P., Elachi, C., Gim, Y., Kirk, R., Lewis, K., Lopes, R., Lorenz, R., Lunine, J., Mitchell, K., Mitri, G., Stofan, E., Wall, S., 2008. Hydrocarbon lakes on Titan: distribution and interaction with a porous regolith. Geophysical Research Letters 35, L09204.
Hayes, A., Aharonson, O., Lunine, J., Kirk, R.L., Zebker, H.A., Wye, L.C., Lorenz, R.D., Turtle, E., Paillou, P., Mitri, G., Wall, S.D., Stofan, E.R., Mitchell, K.L., Elachi, C., the Cassini RADAR Team, 2011. Transient surface liquid in Titan's polar regions from Cassini. Icarus 211 (1), 655–671. doi:10.1016/j.icarus.2010.08.017.
Heslop, S.E., Wilson, L., Pinkerton, H., Head, J.W., 1989. Dynamics of a confined lava flow on Kilauea volcano, Hawaii. Bulletin of Volcanology 51, 415–432.
Howard, A.D., McLane III, C.F., 1988. Erosion of cohesionless sediment by groundwater seepage. Water Resources Research 24, 1659–1674.
Hueso, R., Sánchez-Lavega, A., 2006. Methane storms on Saturn's moon Titan. Nature 442, 428–431.
Jaumann, R., Brown, R.H., Stephan, K., Barnes, J.W., Soderblom, L.A., Sotin, C., Le Mouélic, S., Clark, R.N., Soderblom, J., Buratti, B.J., Wagner, R., McCord, T.B., Rodriguez, S., Baines, K.H., Cruikshank, D.P., Nicholson, P.D., Griffith, C.A., Langhans, M., Lorenz, R.D., 2008. Fluvial erosion and post-erosional processes on Titan. Icarus 197, 526–538.
Jaumann, R., Kirk, R., Lorenz, R., Lopes, R., Stofan, E., Turtle, E., Keller, U., Wood, C.A., Sotin, C., Soderblom, L.A., Tomasko, M., 2009. Geology and surface processes on Titan. In: Brown, R.H., Lebreton, J.-P., Waite, J.H. (Eds.), Titan from Cassini-Huygens. Springer, pp. 75–140.
Jaumann, R., Nass, A., Tirsch, D., Reiss, D., Neukum, G., 2010. The western Libya Montes valley system on Mars: evidence for episodic and multi-genetic erosion events during the Martian history. Earth and Planetary Science Letters 294, 272–290.
Jaumann, R., Stephan, K., Brown, R.H., Buratti, B.J., Clark, R.N., McCord, T.B., Coradini, A., Capaccioni, F., Filacchione, G., Cerroni, P., Baines, K.H., Bellucci, G., Bibring, J., Combes, M., Cruikshank, D.P., Drossart, P., Formisano, V., Langevin, Y., Matson, D.L., Nelson, R.M., Nicholson, P.D., Sicardy, B., Sotin, C., Soderblom, L.A., Griffith, C., Matz, K., Roatsch, T., Scholten, F., Porco, C.C., 2006. High-resolution CASSINI-VIMS mosaics of Titan and the icy Saturnian satellites. Planetary and Space Science 54, 1146–1155.
Kirk, R.L., Howington-Kraus, E., Mitchell, K.L., Hensley, S., Stiles, B.W., the Cassini RADAR Team, 2007. First Stereoscopic Radar Images of Titan. In: Lunar and Planetary Institute Science Conference Abstracts, vol. 38, p. 1427.
Knight, J.F., Lunetta, R.S., 2003. An experimental assessment of minimum mapping unit size. IEEE Transactions on Geoscience and Remote Sensing 41, 2132–2134.
Komar, P.D., 1979. Comparisons of the hydraulics of water flows in Martian outflow channels with flows of similar scale on Earth. Icarus 37, 156–181.
Komatsu, G., 2007. Rivers in the Solar System: water is not the only fluid flow on planetary bodies. Geography Compass 3 (3), 480–502.
Komatsu, G., Baker, V.R., 1996. Channels in the solar system. Planetary and Space Science 44, 801–815.
Lamb, M.P., Dietrich, W.E., Aciego, S.M., DePaolo, D.J., Manga, M., 2008. Formation of Box Canyon, Idaho, by megaflood: implications for seepage erosion on Earth and Mars. Science 320, 1067–1070.
Lamb, M.P., Howard, A.D., Johnson, J., Whipple, K.X., Dietrich, W.E., Perron, J.T., 2006. Can springs cut canyons into rock? Journal of Geophysical Research (Planets) 111, E07002.
Langhans, M., Jaumann, R., Stephan, K., Brown, R.H., Buratti, B.J., Clark, R., Baines, K.H., Nicholson, P.D., Lorenz, R., 2010. Spectral properties of fluvial terrain on Titan: an update. In: European Planetary Science Congress Abstracts, vol. 5, EPSC2010-714.
Le Corre, L., Le Mouélic, S., Sotin, C., Combe, J.-P., Rodriguez, S., Barnes, J.W., Brown, R.H., Buratti, B.J., Jaumann, R., Soderblom, J., Soderblom, L.A., Clark, R., Baines, K.H., Nicholson, P.D., 2009. Analysis of a cryolava flow-like feature on Titan. Planetary and Space Science 57, 870–879.
Le Gall, A., Janssen, M.A., Paillou, P., Lorenz, R.D., Wall, S.D., 2010. the Cassini RADAR team, 2010. Radar-bright channels on Titan. Icarus 207, 948–958. URL: 〈http://wwwsciencedirect.com/science/article/B6WGF-4Y34WFH-8/2/da5afb263ff2b2428e26f520fa3af0e3〉.
Le Mouélic, S., Paillou, P., Janssen, M.A., Barnes, J.W., Rodriguez, S., Sotin, C., Brown, R.H., Baines, K.H., Buratti, B.J., Clark, R.N., Crapeau, M., Encrenaz, P.J., Jaumann, R., Geudtner, D., Paganelli, F., Soderblom, L., Tobie, G., Wall, S., 2008. Mapping and interpretation of Sinlap crater on Titan using Cassini VIMS and RADAR data. Journal of Geophysical Research (Planets) 113, E04003.
Lopes, R.M.C., Stofan, E.R., Peckyno, R., Radebaugh, J., Mitchell, K.L., Mitri, G., Wood, C.A., Kirk, R.L., Wall, S.D., Lunine, J.I., Hayes, A., Lorenz, R., Farr, T., Wye, L., Craig, J., Ollerenshaw, R.J., Janssen, M., Legall, A., Paganelli, F., West, R., Stiles, B., Callahan, P., Anderson, Y., Valora, P., Soderblom, L., 2010. the Cassini RADAR Team, 2010. Distribution and interplay of geologic processes on Titan from Cassini radar data. Icarus 205, 540–558. URL: 〈http://wwwsciencedirect.com/science/article/B6WGF-4X2JSXX-1/2/fdf2c4732930d84159cc61b9378dab86〉.
Lorenz, R.D., 2000. The weather on Titan. Science 290 (5491), 467–468 URL: 〈http://www.sciencemag.org〉.
Lorenz, R.D., Brown, M.E., Flasar, F.M., 2009. Seasonal change on Titan. In: Brown, R.H., Lebreton, J.-P., Waite, J.H. (Eds.), Titan from Cassini-Huygens. Springer, pp. 353–372.
Lorenz, R.D., Green, J.R., Wood, C.A., Coustenis, A., Ori, G.G., Paillou, P., Yelle, R., Bolton, S.J., Baines, K.H., Terrile, R.J., Gurwell, M.A., Griffith, C.A., Wong, A.-S., Rages, K.A., 2002. Titan. In: Sykes, M.V. (Ed.), The Future of Solar System Exploration (2003–2013)—First Decadal Study Contributions, Astronomical Society of the Pacific Conference Series, vol. 272, pp. 253–261.
Lorenz, R.D., Griffith, C.A., Lunine, J.I., McKay, C.P., Rennò, N.O., 2005. Convective plumes and the scarcity of Titan's clouds. Geophysical Research Letters 32, L01201.
Lorenz, R.D., Kraal, E., Asphaug, E., Thomson, R.E., 2003. The Seas of Titan. EOS Transactions 84, 125–131.
Lorenz, R.D., Lopes, R.M., Paganelli, F., Lunine, J.I., Kirk, R.L., Mitchell, K.L., Soderblom, L.A., Stofan, E.R., Ori, G., Myers, M., Miyamoto, H., Radebaugh, J., Stiles, B., Wall, S.D., Wood, C.A., 2008. the Cassini RADAR Team, 2008. Fluvial channels on Titan: initial Cassini RADAR observations. Planetary and Space Science 56, 1132–1144.
Lorenz, R.D., Lunine, J.I., 1996. Erosion on Titan: past and present. Icarus 122, 79–91.
Lorenz, R.D., Wall, S., Radebaugh, J., Boubin, G., Reffet, E., Janssen, M., Stofan, E., Lopes, R., Kirk, R., Elachi, C., Lunine, J., Mitchell, K., Paganelli, F., Soderblom, L., Wood, C., Wye, L., Zebker, H., Anderson, Y., Ostro, S., Allison, M., Boehmer, R., Callahan, P., Encrenaz, P., Ori, G.G., Francescetti, G., Gim, Y., Hamilton, G., Hensley, S., Johnson, W., Kelleher, K., Muhleman, D., Picardi, G., Posa, F., Roth, L., Seu, R., Shaffer, S., Stiles, B., Vetrella, S., Flamini, E., West, R., 2006. The sand seas of Titan: Cassini RADAR observations of longitudinal dunes. Science 312, 724–727.
Lunine, J.I., Atreya, S.K., 2008. The methane cycle on Titan. Nature Geoscience 1, 159–164.
Lunine, J.I., Elachi, C., Wall, S.D., Janssen, M.A., Allison, M.D., Anderson, Y., Boehmer, R., Callahan, P., Encrenaz, P., Flamini, E., Franceschetti, G., Gim, Y., Hamilton, G., Hensley, S., Johnson, W.T.K., Kelleher, K., Kirk, R.L., Lopes, R.M., Lorenz, R., Muhleman, D.O., Orosei, R., Ostro, S.J., Paganelli, F., Paillou, P., Picardi, G., Posa, F., Radebaugh, J., Roth, L.E., Seu, R., Shaffer, S., Soderblom, L.A., Stiles, B., Stofan, E.R., Vetrella, S., West, R., Wood, C.A., Wye, L., Zebker, H., Alberti, G., Karkoschka, E., Rizk, B., McFarlane, E., See, C., Kazeminejad, B., 2008a. Titan's diverse landscapes as evidenced by Cassini RADAR's third and fourth looks at Titan. Icarus 195, 415–433 URL: 〈http://www.sciencedirect.com/science/article/B6WGF-4RM1KY4-2/2/60dc6a26071d138a4b59304d0814ae06〉.
Lunine, J.I., Lorenz, R.D., 2009. Rivers, lakes, dunes, and rain: crustal processes in Titan's methane cycle. Annual Review of Earth and Planetary Sciences 37, 299–320.
Lunine, J.I., Mitri, G., Elachi, C., Stofan, E.R., Lorenz, R.D., Kirk, R.L., Michell, K., Lopes, R.M.C., Wood, C.A., Radebaugh, J., Wall, S.D., Soderblom, L.A., Pallou, P., Farr, T., Stiles, B., Callahan, P., the Cassini Radar Team, 2008b. Lack of south polar methane lakes on Titan. In: Lunar and Planetary Institute Science Conference Abstracts, vol. 39, p. 1637.
Lunine, J.I., Stevenson, D.J., Yung, Y.L., 1983. Ethane ocean on Titan. Science 222, 1229–1230.
Mangold, N., Quantin, C., Ansan, V., Delacourt, C., Allemand, P., 2004. Evidence for precipitation on Mars from dendritic valleys in the Valles Marineris area. Science 305, 78–81.
McCord, T.B., Hansen, G.B., Buratti, B.J., Clark, R.N., Cruikshank, D.P., D'Aversa, E., Griffith, C.A., Baines, E.K.H., Brown, R.H., Dalle Ore, C.M., Filacchione, G., Formisano, V., Hibbitts, C.A., Jaumann, R., Lunine, J.I., Nelson, R.M., Sotin, C., 2006. the Cassini VIMS Team, 2006. Composition of Titan's surface from Cassini VIMS. Planetary and Space Science 54, 1524–1539.
Mitchell, J.L., Pierrehumbert, R.T., Frierson, D.M.W., Caballero, R., 2009. The impact of methane thermodynamics on seasonal convection and circulation in a model Titan atmosphere. Icarus 203, 250–264.
Mitchell, K.L., Wall, S.D., Stofan, E.R., Lopes, R.M.C., Janssen, M., Stiles, B., Paillou, P., Mitri, G., Lunine, J., Ostro, S., Lorenz, R.D., Farr, T.G., Kirk, R.L., Radebaugh, J., the Cassini

Radar Science Team, 2007. Titan's north polar lakes as observed by Cassini Radar: an update. In: Ices, Oceans, and Fire: Satellites of the Outer Solar System, p. 6042.
Ori, G.G., Marinangeli, L., Baliva, A., Bressan, M., Strom, R.G., 1998. Fluid dynamics of liquids on Titans surface. Planetary and Space Science 46, 1417–1421.
Paganelli, F., Elachi, C., Lopes, R.M., West, R.A., Stiles, B., Janssen, M.A., Stofan, E.R., Wood, C.A., Lorenz, R.D., Lunine, J., Kirk, R.L., Roth, L.E., Wall, S.D., Soderblom, L.A., the Cassini Radar Science Team, 2005. Channels and fan-like features on Titan surface imaged by the Cassini RADAR. In: Lunar and Planetary Institute Science Conference Abstracts, vol. 36, p. 2150.
Perron, J.T., Lamb, M.P., Koven, C.D., Fung, I.Y., Yager, E., Ádámkovics, M., 2006. Valley formation and methane precipitation rates on Titan. Journal of Geophysical Research (Planets) 111, E11001.
Porco, C.C., Baker, E., Barbara, J., Beurle, K., Brahic, A., Burns, J.A., Charnoz, S., Cooper, N., Dawson, D.D., Del Genio, A.D., Denk, T., Dones, L., Dyudina, U., Evans, M.W., Fussner, S., Giese, B., Grazier, K., Helfenstein, P., Ingersoll, A.P., Jacobson, R.A., Johnson, T.V., McEwen, A., Murray, C.D., Neukum, G., Owen, W.M., Perry, J., Roatsch, T., Spitale, J., Squyres, S., Thomas, P., Tiscareno, M., Turtle, E.P., Vasavada, A.R., Veverka, J., Wagner, R., West, R., 2005. Imaging of Titan from the Cassini spacecraft. Nature 434, 159–168.
Radebaugh, J., Lorenz, R.D., Kirk, R.L., Lunine, J.I., Stofan, E.R., Lopes, R.M.C., Wall, S.D., 2007. the Cassini Radar Team, 2007. Mountains on Titan observed by Cassini Radar. Icarus 192, 77–91.
Radebaugh, J., Lorenz, R.D., Lunine, J.I., Wall, S.D., Boubin, G., Reffet, E., Kirk, R.L., Lopes, R.M., Stofan, E.R., Soderblom, L., Allison, M., Janssen, M., Paillou, P., Callahan, P., Spencer, C., 2008. the Cassini Radar Team, 2008. Dunes on Titan observed by Cassini Radar. Icarus 194, 690–703.
Rannou, P., Montmessin, F., Hourdin, F., Lebonnois, S., 2006. The latitudinal distribution of clouds on Titan. Science 311, 201–205.
Rodriguez, S., Le Mouélic, S., Rannou, P., Tobie, G., Baines, K.H., Barnes, J.W., Griffith, C.A., Hirtzig, M., Pitman, K.M., Sotin, C., Brown, R.H., Buratti, B.J., Clark, R.N., Nicholson, P.D., 2009. Global circulation as the main source of cloud activity on Titan. Nature 459, 678–682.
Rodriguez, S., Le Mouélic, S., Sotin, C., Clénet, H., Clark, R.N., Buratti, B., Brown, R.H., McCord, T.B., Nicholson, P.D., Baines, K.H., 2006. the VIMS Science Team, 2006. Cassini/VIMS hyperspectral observations of the Huygens Landing Site on Titan. Planetary and Space Science 54, 1510–1523.
Sahlin, E.A.U., Glasser, N.F., Jansson, K.N., Hambrey, M.J., 2009. Connectivity analyses of valley patterns indicate preservation of a preglacial fluvial valley system in the Dyfi basin, Wales. In: Proceedings of the Geologists' Association 120, pp. 114–127.
Schowengerdt, R.A., 1997. Remote Sensing—Models and Methods for Image Processing, second ed. Academic Press.
Schumm, S.A., Boyd, K.F., Wolff, C.G., Spitz, W.J., 1995. A ground-water sapping landscape in the Florida Panhandle. Geomorphology 12, 281–297.
Smith, P.H., Lemmon, M.T., Lorenz, R.D., Sromovsky, L.A., Caldwell, J.J., Allison, M.D., 1996. Titan's surface, revealed by HST imaging. Icarus 119, 336–349.
Soderblom, J.M., Brown, R.H., Soderblom, L.A., Barnes, J.W., Jaumann, R., Mouélic, S.L., Sotin, C., Stephan, K., Baines, K.H., Buratti, B.J., Clark, R.N., Nicholson, P.D., 2010. Geology of the Selk crater region on Titan from Cassini VIMS observations. Icarus 208, 905–912. URL: 〈http://wwwsciencedirect.com/science/article/B6WGF-4YK7J6D-3/2/13cb87bc492353d664d6d8bc83bc524e〉.
Soderblom, L.A., Barnes, J.W., Brown, R.H., Clark, R.N., Jannsen, M.A., McCord, T.B., Niemann, H.B., Tomasko, M.G., 2009. Composition of Titan's surface. In: Brown, R.H., Lebreton, J.-P., Waite, J.H. (Eds.), Titan from Cassini-Huygens. Springer, pp. 141–176.
Soderblom, L.A., Kirk, R.L., Lunine, J.I., Anderson, J.A., Baines, K.H., Barnes, J.W., Barrett, J.M., Brown, R.H., Buratti, B.J., Clark, R.N., Cruikshank, D.P., Elachi, C., Janssen, M.A., Jaumann, R., Karkoschka, E., Le Mouélie, S., Lopes, R.M., Lorenz, R.D., McCord, T.B., Nicholson, P.D., Radebaugh, J., Rizk, B., Sotin, C., Stofan, E.R., Sucharski, T.L., Tomasko, M.G., Wall, S.D., 2007a. Correlations between Cassini VIMS spectra and RADAR SAR images: implications for Titan's surface composition and the character of the Huygens Probe Landing Site. Planetary and Space Science 55, 2025–2036.
Soderblom, L.A., Tomasko, M.G., Archinal, B.A., Becker, T.L., Bushroe, M.W., Cook, D.A., Doose, L.R., Galuszka, D.M., Hare, T.M., Howington-Kraus, E., Karkoschka, E., Kirk, R.L., Lunine, J.I., McFarlane, E.A., Redding, B.L., Rizk, B., Rosiek, M.R., See, C., Smith, P.H., 2007b. Topography and geomorphology of the Huygens Landing Site on Titan. Planetary and Space Science 55, 2015–2024.
Stephan, K., Jaumann, R., Brown, R.H., Soderblom, J.M., Soderblom, L.A., Barnes, J.W., Sotin, C., Griffith, C.A., Kirk, R.L., Baines, K.H., Buratti, B.J., Clark, R.N., Lytle, D.M., Nelson, R.M., Nicholson, P.D., 2010. Specular reflection on Titan: liquids in Kraken Mare. Geophysical Research Letters 37, L07104.
Stephan, K., Jaumann, R., Karkoschka, E., Kirk, R., Barnes, J.W., Tomasko, M.G., Turtle, E.P., Le Corre, L., Langhans, M., Le Mouélic, S., Lorenz, R.D., Perry, J., 2009. Mapping products of Titan's surface. In: Brown, R.H., Lebreton, J.-P., Waite, J.H. (Eds.), Titan from Cassini-Huygens. Springer, pp. 489–510.
Stevenson, D.J., 1992. Interior of Titan. In: Kaldeich, B. (Ed.), Symposium on Titan, vol. 338. ESA Special Publication, pp. 29–33.
Stevenson, D.J., Potter, B.E., 1986. Titan's latitudinal temperature distribution and seasonal cycle. Geophysical Research Letters 13, 93–96.
Stofan, E.R., Elachi, C., Lunine, J.I., Lorenz, R.D., Stiles, B., Mitchell, K.L., Ostro, S., Soderblom, L., Wood, C., Zebker, H., Wall, S., Janssen, M., Kirk, R., Lopes, R., Paganelli, F., Radebaugh, J., Wye, L., Anderson, Y., Allison, M., Boehmer, R., Callahan, P., Encrenaz, P., Flamini, E., Francescetti, G., Gim, Y., Hamilton, G., Hensley, S., Johnson, W.T.K., Kelleher, K., Muhleman, D., Paillou, P., Picardi, G., Posa, F., Roth, L., Seu, R., Shaffer, S., Vetrella, S., West, R., 2007. The lakes of Titan. Nature 445, 61–64.
Stofan, E.R., Lunine, J.I., Lopes, R., Paganelli, F., Lorenz, R.D., Wood, C.A., Kirk, R., Wall, S., Elachi, C., Soderblom, L.A., Ostro, S., Janssen, M., Radebaugh, J., Wye, L., Zebker, H., Anderson, Y., Allison, M., Boehmer, R., Callahan, P., Encrenaz, P., Flamini, E., Francescetti, G., Gim, Y., Hamilton, G., Hensley, S., Johnson, W.T.K., Kelleher, K., Muhleman, D., Picardi, G., Posa, F., Roth, L., Seu, R., Shaffer, S., Stiles, B., Vetrella, S., West, R., 2006. Mapping of Titan: results from the first Titan radar passes. Icarus 185, 443–456.
Thompson, W.R., Squyres, S.W., 1990. Titan and other icy satellites: dielectric properties of constituent materials and implications for radar sounding. Icarus 86, 336–354.
Tokano, T., 2009. Impact of seas/lakes on polar meteorology of Titan: simulation by a coupled GCM-Sea model. Icarus 204, 619–636.
Tokano, T., McKay, C.P., Neubauer, F.M., Atreya, S.K., Ferri, F., Fulchignoni, M., Niemann, H.B., 2006. Methane drizzle on Titan. Nature 442, 432–435.
Tomasko, M.G., Archinal, B., Becker, T., Bézard, B., Bushroe, M., Combes, M., Cook, D., Coustenis, A., de Bergh, C., Dafoe, L.E., Doose, L., Douté, S., Eibl, A., Engel, S., Gliem, F., Grieger, B., Holso, K., Howington-Kraus, E., Karkoschka, E., Keller, H.U., Kirk, R., Kramm, R., Küppers, M., Lanagan, P., Lellouch, E., Lemmon, M., Lunine, J., McFarlane, E., Moores, J., Prout, G.M., Rizk, B., Rosiek, M., Rueffer, P., Schröder, S.E., Schmitt, B., See, C., Smith, P., Soderblom, L., Thomas, N., West, R., 2005. Rain, winds and haze during the Huygens probe's descent to Titan's surface. Nature 438, 765–778.
Turtle, E.P., Perry, J.E., Hayes, A.G., McEwen, A.S. Shoreline retreat at Titan's Ontario Lacus and Arrakis Planitia from Cassini Imaging Science Subsystem observations. Icarus, in press, doi:10.1016/j.icarus.2011.02.005.
von Bertalanffy, L., 1968. General System Theory. George Braziller Inc., New York.
Wall, S., Hayes, A., Bristow, C., Lorenz, R., Stofan, E., Lunine, J., Le Gall, A., Janssen, M., Lopes, R., Wye, L., Soderblom, L., Paillou, P., Aharonson, O., Zebker, H., Farr, T., Mitri, G., Kirk, R., Mitchell, K., Notarnicola, C., Casarano, D., Ventura, B., 2010. Active shoreline of Ontario Lacus, Titan: a morphological study of the lake and its surroundings. Geophysical Research Letters 37, L05202.
Williams, R.M.E., Phillips, R.J., 2001. Morphometric measurements of martian valley networks from Mars Orbiter Laser Altimeter (MOLA) data. Journal of Geophysical Research (Planets) 106, 23737–23752.
Wood, C.A., Lorenz, R., Kirk, R., Lopes, R., Mitchell, K., Stofan, E., 2010. the Cassini RADAR Team, 2010. Impact craters on Titan. Icarus 206, 334–344.
Wye, L.C., Zebker, H.A., Lorenz, R.D., 2009. Smoothness of Titan's Ontario Lacus: constraints from Cassini Radar specular reflection data. Geophysical Research Letters 36, L16201.